

Report Date: April 26, 2004

Semi-Annual Technical Progress Report

**INVESTIGATION OF EFFICIENCY IMPROVEMENTS DURING CO₂
INJECTION IN HYDRAULICALLY AND NATURALLY FRACTURED
RESERVOIRS**

DOE Contract No.: DE-FC26-01BC15361

Harold Vance Department of Petroleum Engineering
Texas A& M University
3116 TAMU
College Station, TX 77843-3116
(979) 845-2241

Contract Date:	September 28, 2001
Anticipated Completion Date:	September 27, 2004

Principal Investigator:	David S. Schechter Harold Vance Department of Petroleum Engineering
-------------------------	---

Contracting Officer's Representative:	Dan Ferguson National Petroleum Technology Office
---------------------------------------	--

Report Period:	Nov 1, 2003-April 1, 2004
----------------	---------------------------

US/DOE Patent Clearance is not required prior to the publication of this document.

DISCLAIMER

This report was prepared as an account of work sponsored by an agency of the United States Government. Neither the United States Government nor any agency thereof, nor any their employees, makes any warranty, express or implied, or assumes any legal liability or responsibility for the accuracy, completeness, or usefulness of any information, apparatus, product, or process disclosed, or represents that its use would not infringe privately owned rights. Reference herein to any specific commercial product, process, or service by trade name, trademark, manufacturer, or otherwise does not necessarily constitute or imply its endorsement, recommendation, or favoring by the United States Government or any agency thereof. The views and opinions of authors expressed herein do not necessarily state or reflect those of the United States Government or any agency thereof.

ABSTRACT

This report describes the work performed during the second year of the project, “Investigating of Efficiency Improvements during CO₂ Injection in Hydraulically and Naturally Fractured Reservoirs.” The objective of this project is to perform unique laboratory experiments with artificial fractured cores (AFCs) and X-ray CT to examine the physical mechanisms of bypassing in HFR and NFR that eventually result in less efficient CO₂ flooding in heterogeneous or fracture-dominated reservoirs. To achieve this objective, in this period we concentrated our effort on investigating the effect of CO₂ injection rates in homogeneous and fractured cores on oil recovery and a strategy to mitigate CO₂ bypassing in a fractured core. The following headings outline the abstract that appears in this report.

Application of X-Ray CT for Investigating Effect of CO₂ Injection Rates on Oil Recovery

Fractured reservoirs have always been considered poor candidates for enhanced oil recovery. This is mainly due to the complexities involved in predicting performance in such reservoirs. A good understanding of multiphase flow in fractures is important to reduce oil bypass and increase recovery in these reservoirs. In this report, CO₂ flooding experiments in homogeneous and fractured rocks were performed using X-ray CT Scanner to determine the effect of CO₂ injection rates on oil recovery. We found that injection rates played an important role in the recovery process, more so in the presence of fractures. At high injection rates, we observed faster CO₂ breakthrough and higher oil bypass than at low injection rates. Low injection rates can thus lead to an increase in recovery, although not attractive from an economic point of view.

Possible Strategies to Mitigate CO₂ Flooding Bypassing Mechanisms in Fracture-Dominated Reservoirs.

This report is a continuation of our previous work in order to find possible strategies to mitigate CO₂ flooding bypassing mechanism. Since, very low injection rates are not attractive from an economic point of view. Hence, we injected viscosified water to reduce the mobility of CO₂, similar to the WAG process. We found that the CO₂ breakthrough time reduced significantly and a much higher recovery was obtained. We measured average saturations from the CT scans and compared them with the saturation from the effluent data. We found that they are in a good agreement, thus, it validates the result obtained from the X-ray CT.

TABLE OF CONTENTS

DISCLAIMER.....	ii
ABSTRACT.....	iii
TABLE OF CONTENTS.....	iv
LIST OF TABLES.....	vi
LIST OF FIGURES	vii
ACKNOWLEDGMENTS	x
EXECUTIVESUMMARY.....	xi
 I. Application of X-Ray CT for Investigating Effect of CO ₂ Injection Rates on Oil Recovery	 1
1.1 Introduction.....	1
1.2 Background.....	3
1.3 Experimental Setup.....	5
1.3.1 Injection System.....	5
1.3.2 Coreflood Cell.....	5
1.3.3 X-Ray CT Scanner.....	6
1.3.4 Production System	6
1.3.5 Data Acquisition System.....	6
1.4 Experimental Procedure.....	7
1.5 Results and Discussion	9
1.5.1 High Injection Rate.....	9
1.5.2 Low Injection Rate.....	19
1.5.3 Fractured Core	28
1.6 Conclusions.....	33
1.7 References.....	33
 II. Possible Strategies to Mitigate CO ₂ Flooding Bypassing Mechanisms in Fracture- Dominated Reservoirs.....	 36
2.1 Introduction.....	36
2.2 Experimental Setup.....	37
2.3 Experimental Procedure.....	38

2.4 Results and Discussion	39
2.4.1 Homogeneous Core Experiments	39
2.4.2 Fractured Core Experiments	41
2.5 Conclusions.....	44
2.6 References.....	45
APPENDIX-A.....	56

LIST OF TABLES

-

LIST OF FIGURES

Figure 1.1 — Phase diagram of CO ₂	3
Figure 1.2 — Density of CO ₂ shows abrupt changes at pressures below critical temperature	4
Figure 1.3 — Density of CO ₂ at experimental conditions.....	5
Figure 1.4 — Schematic of the experimental setup.....	7
Figure 1.5 — Dry core scans with the bright blue scans representing higher CT regions	9
Figure 1.6 — Oil saturated core scans with red color indicating higher CT numbers	10
Figure 1.7 — CO ₂ Injection at 15 minutes shows CO ₂ as a green spot at the center	10
Figure 1.8 — CT Scans at 25 minutes after CO ₂ injection.....	11
Figure 1.9 — CT Scans at 35 minutes after CO ₂ injection.....	11
Figure 1.10 — CT Scans at 60 minutes after CO ₂ injection.....	12
Figure 1.11 — CT scans showing almost 100% CO ₂ saturated cores at 120 minutes	12
Figure 1.12 — CT numbers for dry cores showing a difference of 100 CT numbers for the highest and lowest CT number slices.....	13
Figure 1.13 — CT Numbers for oil saturated core follow same trend as dry core.....	13
Figure 1.14 — Sample plots of CO ₂ injected core images showing a decrease in CT number with increase in CO ₂ saturation	14
Figure 1.15 — CO ₂ saturated cores showing uniform CT numbers	14
Figure 1.16a — Reconstruction of dry core images	15
Figure 1.16b — Reconstruction of oil saturated core images.....	15
Figure 1.16c — CO ₂ injection - 15 minutes	16
Figure 1.16d — CO ₂ injection - 25 minutes	16
Figure 1.16e — CO ₂ injection - 35 minutes	16
Figure 1.16f — CO ₂ injection - 60 minutes.....	17
Figure 1.16g — CO ₂ injection - 120 minutes	17
Figure 1.17a — CO ₂ saturation distribution at 15 minutes after injection	18
Figure 1.17b — CO ₂ saturation distribution at 25 minutes after injection.....	18
Figure 1.17c — CO ₂ saturation distribution at 35 minutes after injection	19
Figure 1.17d — CO ₂ saturation distribution at 60 minutes after injection.....	19

Figure 1.18 — Oil saturated core scans.....	20
Figure 1.18a — Reconstructed image of oil saturated core.....	20
Figure 1.19 — CO ₂ injection - 30 minutes	21
Figure 1.19a — Reconstructed image.....	21
Figure 1.20 — CO ₂ injection - 60 minutes	22
Figure 1.20a — Reconstructed image.....	22
Figure 1.21 — CO ₂ injection - 120 minutes	23
Figure 1.21a — Reconstructed image.....	23
Figure 1.22 — CO ₂ injection - 150 minutes	24
Figure 1.22a — Reconstructed image.....	24
Figure 1.23 — CO ₂ injection -180 minutes (CO ₂ breakthrough)	25
Figure 1.23a — Reconstructed image.....	25
Figure 1.24 — Core with 99% CO ₂ saturation	26
Figure 1.24a — Reconstructed image.....	26
Figure 1.25 — CO ₂ saturations at various slice locations	27
Figure 1.26 — Plot of average CO ₂ saturation in the core with time.....	28
Figure 1.27 — CT scan images of oil saturated, fractured core	29
Figure 1.28 — CT image profile plot for a fractured core.....	29
Figure 1.29 — CT scan images during CO ₂ injection	30
Figure 1.30 — CT image profile plots during CO ₂ injection	31
Figure 1.31 — Ortho reconstruction of oil saturated fractured core.....	31
Figure 1.32a — Reconstruction including the first half of the fracture shows CO ₂ flow (blue color).....	32
Figure 1.32b — Reconstruction including the second half of the fracture face with CO ₂	32
Figure 2.1 — Schematic of the experimental setup.....	47
Figure 2.2 — Cross-Sectional scans taken at various stages during the experiment.....	48
Figure 2.3 — CT number decreases with increase in CO ₂ saturation.	49
Figure 2.4 — Reconstructions of cross-sectional scans for high injection rate case.....	49
Figure 2.5 — Reconstructions of cross-sectional scans for high injection rate case.....	50
Figure 2.6 — CO ₂ saturations along the length of the core at different stages of injection.	51
Figure 2.7 — Higher oil recovery is obtained for lesser pore volumes injected in the low	

injection rate case.....	52
Figure 2.8 — Cross-sectional scans taken during the continuous CO ₂ injection experiment.....	53
Figure 2.9 — Scans taken at water breakthrough where red color indicates water.....	54
Figure 2.10 — Scans taken at various stages of the experiment in the presence of gel.	54
Figure 2.11 — Recovery curves for the various cases showing highest recovery in the presence of gel.	55

ACKNOWLEDGMENTS

Financial support for this work is provided by the United States Department of Energy (NPTO/National Petroleum Technology Office). This support is gratefully acknowledged.

I greatly appreciate diligent efforts from the following individuals who contributed to this project: Erwinsyah Putra helped with the technical part of this research, Deepak Chakravarty and Vivek Muralidharan conducted experimental work on the X-Ray CT scanner as described in Chapters 1 and 2.

EXECUTIVE SUMMARY

This report describes the work performed during the second year of the project, “Investigating of Efficiency Improvements during CO₂ Injection in Hydraulically and Naturally Fractured Reservoirs.” The objective of this project is to perform unique laboratory experiments with artificial fractured cores (AFCs) and X-ray CT to examine the physical mechanisms of bypassing in HFR and NFR that eventually result in less efficient CO₂ flooding in heterogeneous or fracture-dominated reservoirs.

This report provides results of the fifth semi-annual technical progress report that consists of investigating the effect of CO₂ injection rates on oil recovery and a strategy to mitigate CO₂ bypassing in a fractured core. Within the project objective, the specific goals for this period are to (1) determine the effect of CO₂ injection rates on oil recovery and (2) mitigate CO₂ bypass using WAG and polymer gels.

In this report, we present the following work that has been performed to achieve the aforementioned goals. In the first chapter, we investigated the displacement of oil by CO₂ using X-ray CT scanner in homogeneous and fractured cores. We conducted the experiments at various injection rates. We quantified the amount of oil bypass due to the effect of different injection rates. We also investigated the fluid transfer between matrix and fracture media. Important conclusions can be drawn from the work include:

1. Injection rate plays an important role in affecting oil recovery and breakthrough.
2. Early breakthrough and higher oil bypass are observed at high injection rates.
3. Low injection rate gives better sweep and higher recovery, but this is not attractive as the recovery is too slow
4. In a fractured system, fluid flow occurs mainly through the fractures and a considerable amount of time is required for the injection fluid to penetrate the matrix.
5. An alternative method like WAG is necessary to reduce the mobility of CO₂ in the fractured system.

The second chapter is part of our paper that will be presented at the Petroleum Society’s 5th Canadian International Petroleum Conference (55th Annual Technical Meeting), Calgary, Alberta, Canada, June 8 – 10, 2004. The title of the paper is application of X-ray CT for investigation of CO₂ and WAG injection in fractured reservoirs. In this chapter, we investigated CO₂ flow in fractures, in the presence of water as a mobility control agent. We also performed the experiment with adding a cross-linker to the solution to form a gel. We scanned the entire length of the core in order to obtain saturation distributions at various stages during the course of the experiments, which are important to study fluid transport in the matrix and the fracture. Important conclusions can be drawn from the work include:

1. Coreflood experiments using viscosified water confirmed that WAG can delay CO₂ breakthrough and improve recovery. However, leakoff into the porous rock is very high. This leakoff might be much lower in an oil-wet rock but more work is required to establish this.
2. Formation of gel can eliminate the problem of liquid leakoff into the matrix.

3. Using gel for conformance control results in better sweep and higher recoveries. The type and composition of gel to be used in the presence of CO₂ needs more investigation.

Project Fact Sheet

Progress work efforts at Project Fact Sheet are listed in Appendix A.

Chapter I

Application of X-Ray CT for Investigating Effect of CO₂ Injection Rates on Oil Recovery

1.1 Introduction

CO₂ injection has been widely used for recovering oil from reservoirs due to its easy solubility in crude oil and its ability to “swell” the net volume of oil and thereby reduce oil viscosity by a vaporizing-gas-drive mechanism.¹ The success of a CO₂ flood is decided on the basis of mcf of CO₂ injected per barrel of oil recovered, termed “Utilization Factor”. The quantity of hydrocarbons that can be recovered from a reservoir is influenced by several characteristics of the reservoir including reservoir rock properties, reservoir pressure and temperature, physical and compositional properties of the fluid and structural relief, to name a few. However, the predominant factor in deciding the success of a CO₂ flood is the reservoir heterogeneity. Highly heterogeneous reservoirs with variable lateral and vertical relative permeability characteristics can cause potential problems during CO₂ injection. The injection gas tends to finger ahead into areas with high mobility ratios.² This results in the gas forming preferential paths and “bypassing” large volumes of oil. The degree of bypassing is enhanced to a large extent by the presence of natural or hydraulic fractures. In a fractured reservoir, the displacement process is dependent on the fracture-matrix geometry, size and interaction apart from other physical phenomena. Uleberg and Hoier³ suggest that the injection gas tends to flow in the highly permeable fractures, instead of the normally expected displacement path. These fractures are often responsible for early and excessive breakthrough of CO₂, thus greatly affecting the economics of the project.^{4, 5} It therefore becomes essential to understand the complexities involved in the yet unexplored fracture-matrix interactions.

Computerized tomography is a powerful tool that can be used for non-intrusive determination of variables in rock properties and fluid flow visualization. Invented for medical purposes, the CT scanner is now being used for a wide variety of applications.

Many researchers have used CT for rock property determination (Bergosh *et al.*, 1985⁶; Hornapur *et al.*, 1985⁷; Hornapur *et al.*, 1986⁸; Narayanan and Deans, 1987⁹; Jasti *et al.*, 1988¹⁰; Hidajat *et al.*, 2002¹¹). These include study of heterogeneous rocks, fractures, vuggy carbonates and determination of rock properties like porosity and bulk density. Application of X-Ray CT in various core flood experiments has also been discussed by many researchers. MacAllister *et al.*¹² (1990) conducted three-phase oil/water and gas/water experiments using CT scanner to investigate the dependence of relative permeability on wettability. Withjack¹³ (1987) demonstrated the use of X-Ray CT for flow visualization and determination of fluid saturations. Vinegar and Wellington¹⁴ (1987) used CT to visualize three phase fluid flow during miscible and immiscible displacements using CO₂. They used iodated dopant to distinguish between the different phases. They also proposed methods to determine two phase and three phase fluid saturations. Hicks *et al.*¹⁵ (1994) conducted a study of miscible displacements in heterogeneous carbonate cores using X-Ray CT. Apart from these works, there are a few others that deal with investigation of oil bypassing using X-Ray CT. Wellington and Vinegar¹⁶ (1985) tested the use of surfactants for CO₂ mobility control. They concluded that surfactant can prove to be an effective mobility control agent for CO₂. Yamamoto *et al.*¹⁷ (1994) conducted coreflood experiments to analyze the performance CO₂ WAG injection in layered reservoirs. Oshita *et al.*¹⁸ (2000) discussed the possible reasons for early water breakthrough in oil-wet cores. Alajmi and Grader¹⁹ (2000) conducted two-phase oil/water experiments in fractured cores to study oil bypassing caused during waterflooding in fractured porous media.

Although there have been successful field cases of CO₂ injection in fractured reservoirs, there still exist many uncertainties in this area. Hence this study was undertaken to investigate the mechanisms of fluid transfer between the fracture and the matrix. The goals of this study are as follows:

1. Conduct experiments in homogeneous (unfractured) cores and visualize the displacement of oil by CO₂ using the X-Ray CT scanner. Determine fluid saturations at various positions along the length of the core.
2. Determine the effect of injection rate on oil recovery.
3. Fracture the cores and repeat the above experiments at various injection rates.

4. Study fracture-matrix fluid transfer by scanning the entire length of the core after specific pore volumes of CO₂ injection.

1.2 Background

CO₂ can displace oil from reservoirs by various mechanisms. These mechanisms include solution gas drive, immiscible CO₂ drive, hydrocarbon vaporization, direct miscible drive and multiple contact miscible drive²⁰. The recovery of oil by CO₂ flooding is increased due to the following reasons:

1. Reduction in viscosity of oil
2. Swelling of oil
3. Increase in the oil density
4. Vaporization and extraction of portions of crude oil

CO₂ has a critical temperature of 89° F and a critical pressure of 1070 psia (Fig. 1. 1). The extraction of hydrocarbons from oil takes place only above a particular pressure called the Minimum Miscibility Pressure (MMP). This pressure is dependent on a number of factors among which are, the temperature of the oil in the system and the oil composition. As the temperature increases, the density of CO₂ decreases and hence the pressure required for hydrocarbon extraction increases. Also, this pressure increases with the amount of heavier ends present in the oil.

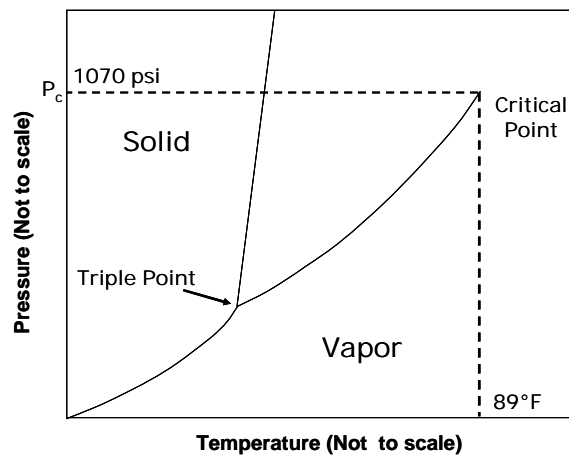


Fig. 1.1 – Phase diagram of CO₂

The objective of our experiments is to first investigate immiscible displacement of oil by CO₂ and extend this to fractures, before proceeding to miscible displacements. Holm and Josendal²⁰ report that for miscible displacement to take place, the density of CO₂ should be at least 0.25 to 0.35 gm/cc. There are various reservoir pressure-temperature combinations that yield these densities. In order to have immiscible displacement, the density of CO₂ must be less than this range. Fig. 1. 2 shows the density of CO₂ for different pressures and temperatures. One important point to be noted is the abrupt shift in densities that occur at pressures below the critical temperature. But the density turns out to be a continuous function of pressure at temperatures above the critical temperature. For our immiscible displacements we decided to maintain the density of CO₂ around 0.15 gm/cc. This density can be achieved at a temperature of 70° F and a pressure of 800 psi. The plot of density versus pressure for this temperature is shown in Fig. 1. 3. At this temperature and pressure, the major mechanisms of oil recovery are swelling of oil, reduction in viscosity and an internal solution gas drive²¹.

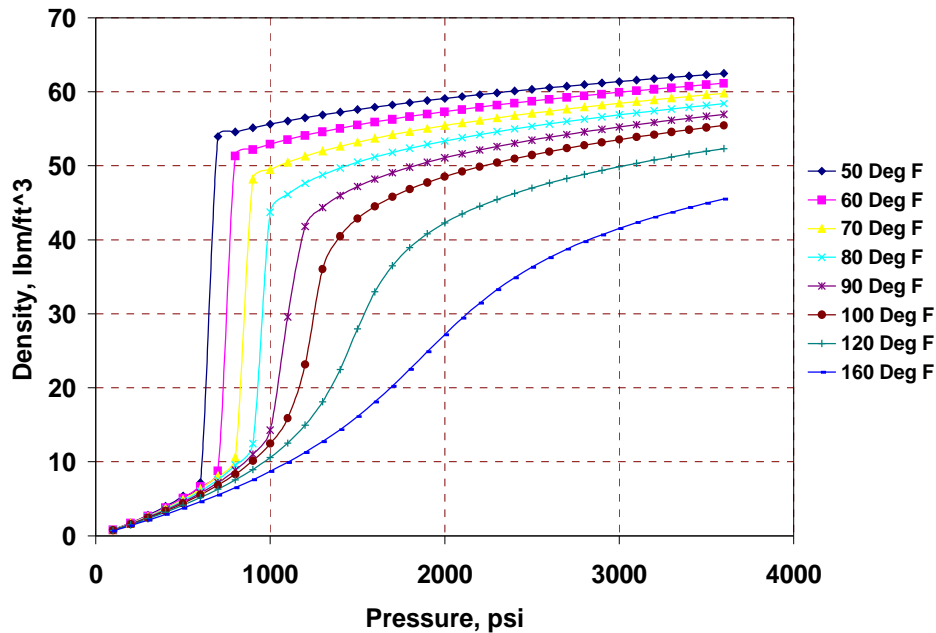


Fig. 1.2 - Density of CO₂ shows abrupt changes at pressures below critical temperature

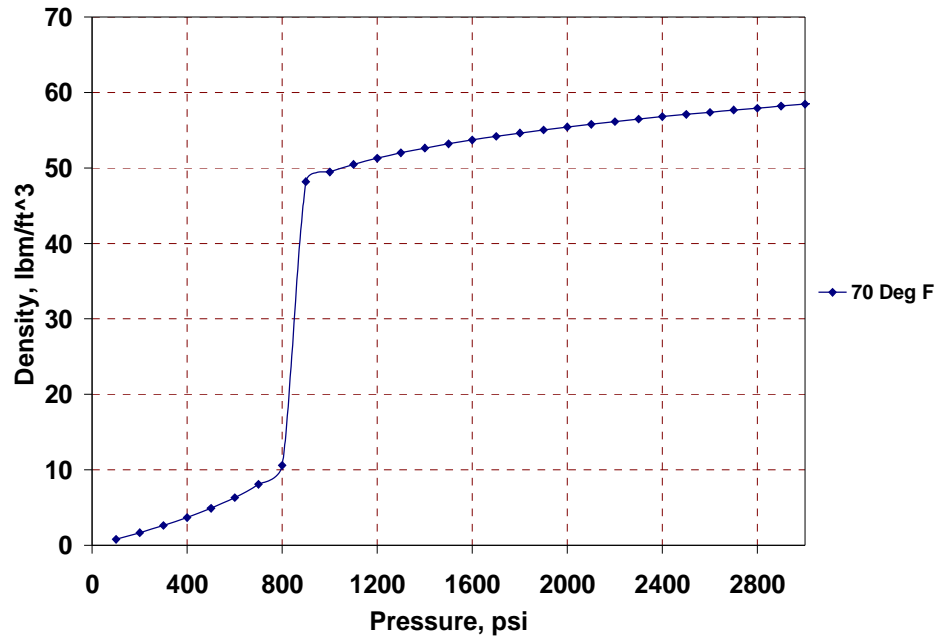


Fig. 1.3 – Density of CO₂ at experimental conditions

1.3 Experimental Setup

The experimental setup consists for five main components – the injection system, the coreflood cell, HD 200 X-Ray CT scanner, the production system and the data acquisition system. A brief description of each of the components is given below.

1.3.1 Injection System

The injection system consists of two accumulators, one for the oil and the other for CO₂. Both the accumulators are connected to an ISCO 5000 D syringe pump. The pump is equipped with a programmable controller using which, it can be run at a constant flow rate or a constant pressure. Water is injected below the piston in the accumulator and this increases the pressure of the fluid above the piston to the desired level. A flow switching valve is used to inject either oil or CO₂ into the coreflood cell.

1.3.2 Coreflood Cell

The core holder measuring 21 in. long is made up of aluminum for use with the CT scanner. It is capable of holding cores up to 1 ft. in length and 1 in. in diameter. A viton

Hassler sleeve surrounds the core and is secured to plungers at the ends of the core holder. The coreflood cell has an inlet for hydraulic oil that is used to apply overburden pressure. A pump is used to pressurize the cell by injecting hydraulic oil into the Hassler sleeve – inner wall annulus and pressures up to 7000 psi can be obtained in this manner.

1.3.3 X-Ray CT Scanner

The X-Ray CT scanner is a fourth generation Universal systems HD 200 system with a resolution of 0.3 mm x 0.3 mm. This scanner can be used to scan a maximum diameter of 48 cm with a maximum scan time of 4 sec per scan. Cross sectional scans of the core sample are made at regular intervals during the experiment. The data obtained from the CTC scanner is transferred to the image processing system installed in a Sun workstation. The cross sectional images can then be used for porosity and saturation determination or reconstructed for flow visualization.

1.3.4 Production System

The outlet end of the core holder is connected to a back pressure regulator which is used to increase pressure in the system. The produced fluid is collected in a graduated cylinder and any gas produced is diverted to the chromatograph and measured using a wet test meter.

1.3.5 Data Acquisition System

Two pressure transducers one each at the inlet and the outlet are used in conjunction with an Omega OMB 55 data acquisition system. The pressures can be read real time from the personal computer connected to the DAQ.

A schematic of the experimental setup is shown in Fig. 1. 4.

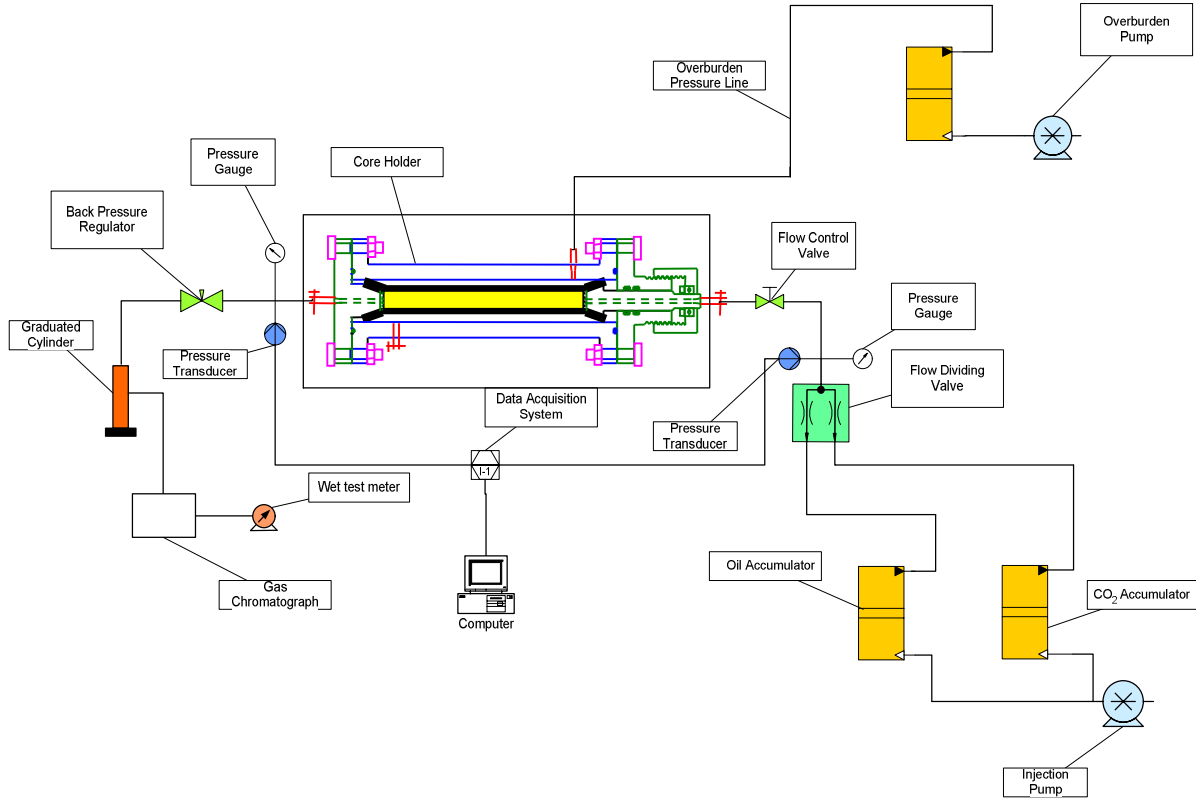


Fig. 1.4 - Schematic of the experimental setup

1.4 Experimental Procedure

The fluid used in the experiment is Soltrol refined oil doped with 1 – IodoHexaDecane. Doping of the oil is required to increase its CT number. It was observed that the CT number for the undoped oil was about -200 whereas oil with dopant concentration of 10% had a CT number of 800 (CT number of air is -1000 and that of water is 0). This dopant was chosen for the experiment considering its molecular structure, which is similar to that of Soltrol. The cores used are Berea cores, which are about 1 inch in diameter and 3.5 inches long. The steps followed in the experiment were as follows:

1. The core is first heated at about 150° F for a sufficient period of time to remove all residual water saturation.
2. The core is then evacuated using a vacuum pump.

3. The evacuated dry core is scanned at a confining pressure of about 750 psi.
4. The core is flooded with CO₂ at the desired temperature and pressure to obtain the scans at 100% CO₂ saturation.
5. The core is then evacuated again in the vacuum chamber.
6. The evacuated core is saturated with doped oil in the vacuum chamber for a period of 48 hours.
7. The oil saturated core is transferred to the aluminum core holder and about 5 pore volumes of oil are injected to ensure complete saturation.
8. The core is then scanned and the fluid saturations are monitored.
9. The backpressure regulator at the outlet is fully closed and the pressure in the core holder is allowed to build up. Care is taken that the overburden pressure is always at least 300 psi higher than the pressure inside the sleeve.
10. Once the desired pressure is reached, oil injection is stopped.
11. The pressure in the CO₂ accumulator is increased to be about 50 psi higher than the pressure in the coreflood cell to prevent back flow of oil.
12. CO₂ is now allowed to enter the coreflood cell and any excess pressure above the desired pressure is released using a valve available for this purpose.
13. Injection is then started at the desired rate.
14. The core is scanned at various times to visualize fluid flow and determine saturations at various times.
15. The experiment is stopped when the produced fluid is 100% CO₂ for a sufficient period of time.

For the fractured core, the experimental procedure is the same except that the core is first fractured and the dry fractured core is scanned to determine the fracture aperture using the calibration curve. The images are then transferred to the image processing software in the form of 256 x 256 pixel matrices containing one slice of the core. The CT numbers at different locations in the slice are then used to determine porosity, saturations etc.

1.5 Results and Discussion

Two experiments were conducted in homogeneous (unfractured) cores: A high injection rate case and a low injection case. The results of the two experiments are discussed below:

1.5.1 High Injection Rate

In this experiment CO₂ was injected at a rate of 0.09 cc/min. The scans were taken at 5 different times: 15 min, 25 min, 35 min, 60 min and 120 min. During the last set of scans, the produced fluid was only CO₂ and almost 99% of the oil in the core had been recovered. A decrease in the CT numbers was observed with an increase in the CO₂ saturation in the core. Figs. 5 to 11 show the CT scans of the dry and oil saturated cores and also scans at various stages of CO₂ injection.

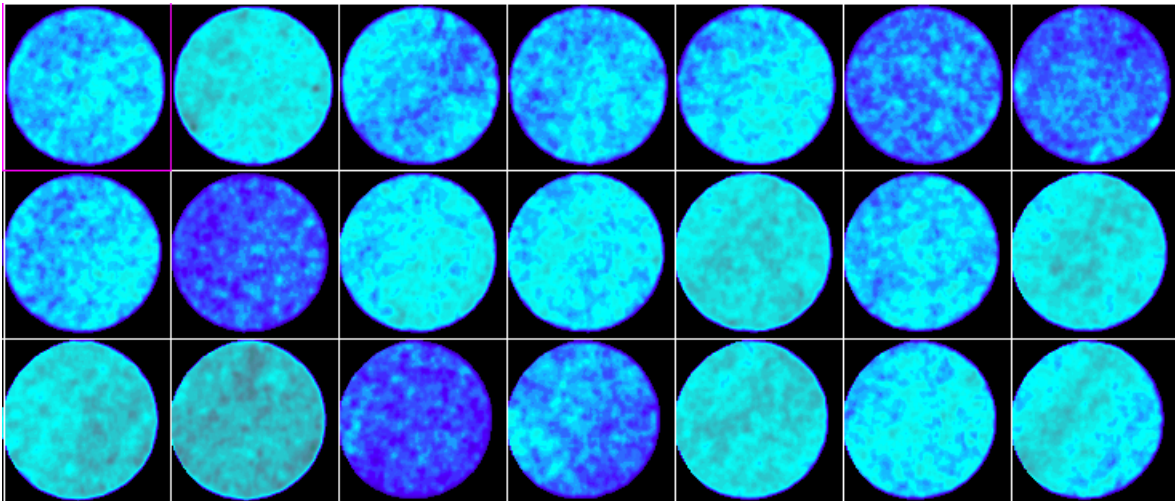


Fig. 1.5 – Dry core scans with the bright blue scans representing higher CT regions

The above figure represents the dry core scans. It can be seen that the core is a fairly homogeneous one. A CT image profile plot of the scans shows that the difference in CT numbers for the highest and lowest CT number scans is about 100. This has been shown later in Fig. 1. 12. This variation in CT number is carried over to the oil saturated cores also where red color represents higher CT numbers (Fig. 1. 13).

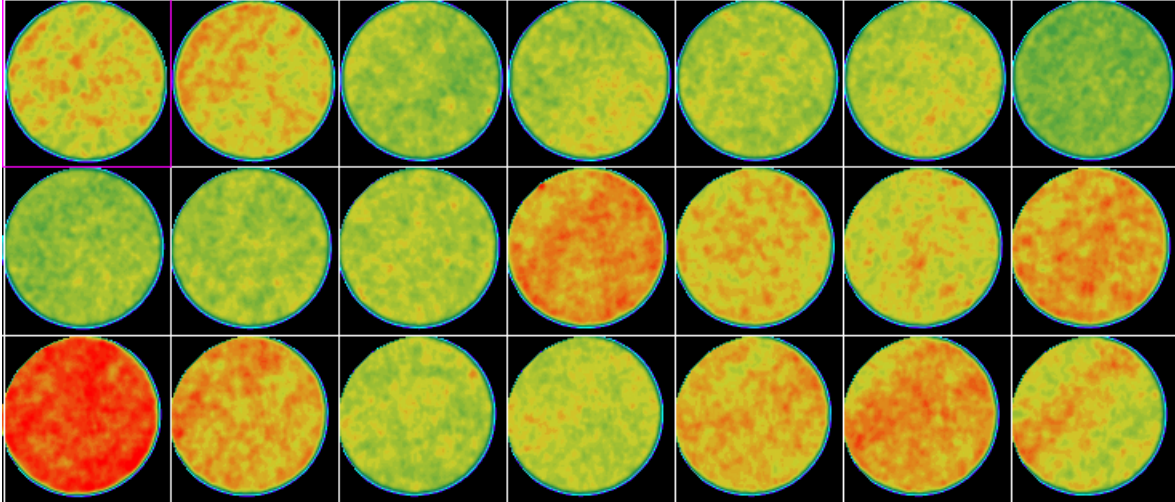


Fig. 1.6 – Oil saturated core scans with red color indicating higher CT numbers

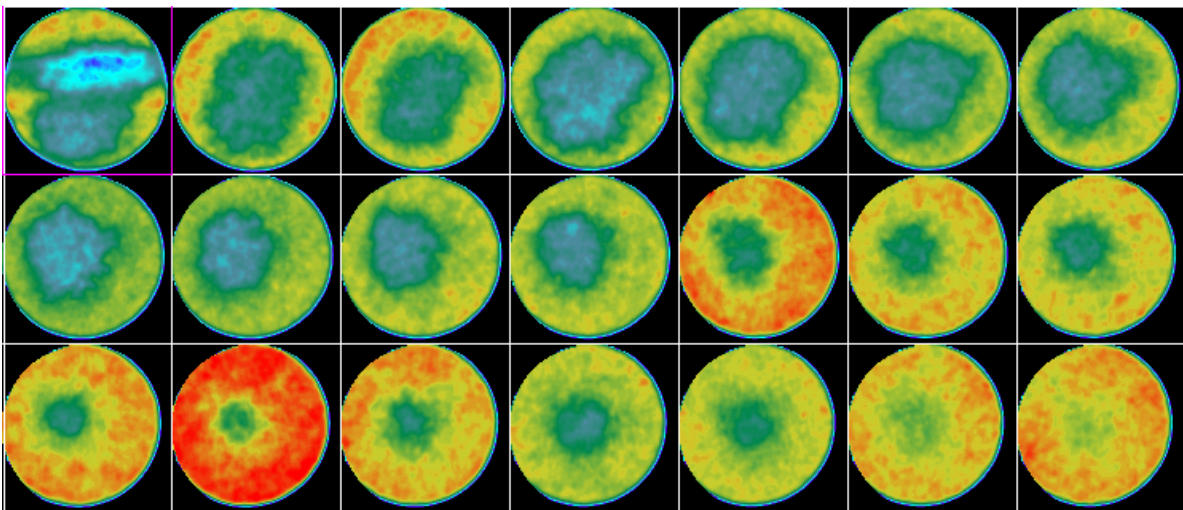


Fig. 1.7 – CO₂ Injection at 15 minutes shows CO₂ as a green spot at the center

Fig. 1. 1 7 shows the cross-sectional scans after 15 minutes of CO₂ injection. It can be observed that there is a small amount of CO₂ observed in the last slice, which indicates that CO₂ has already broken through. Sample CT number plots for CO₂ injected cores have also been shown in the following pages.

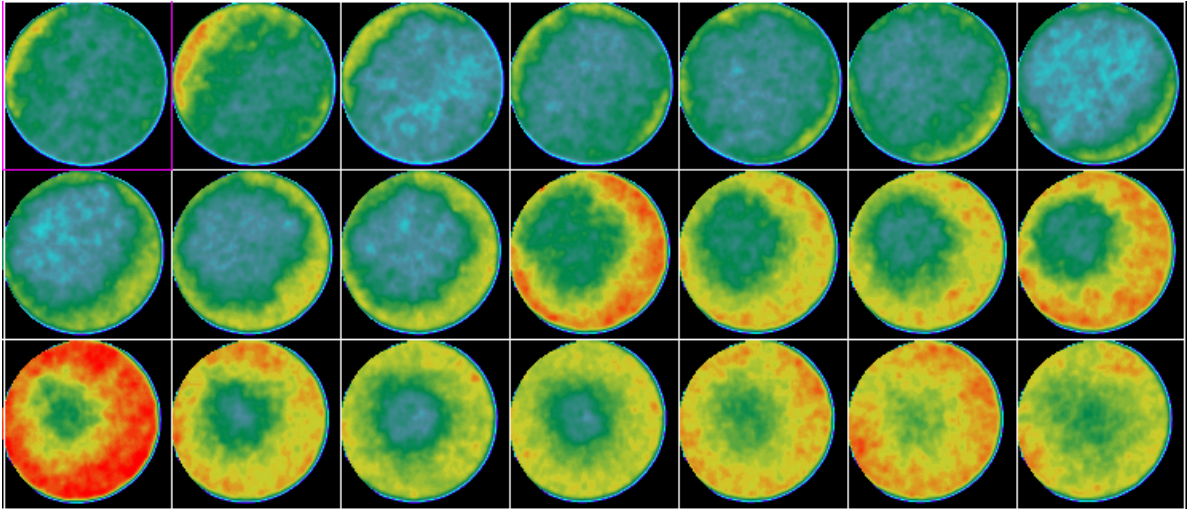


Fig. 1. 8 – CT Scans at 25 minutes after CO₂ injection

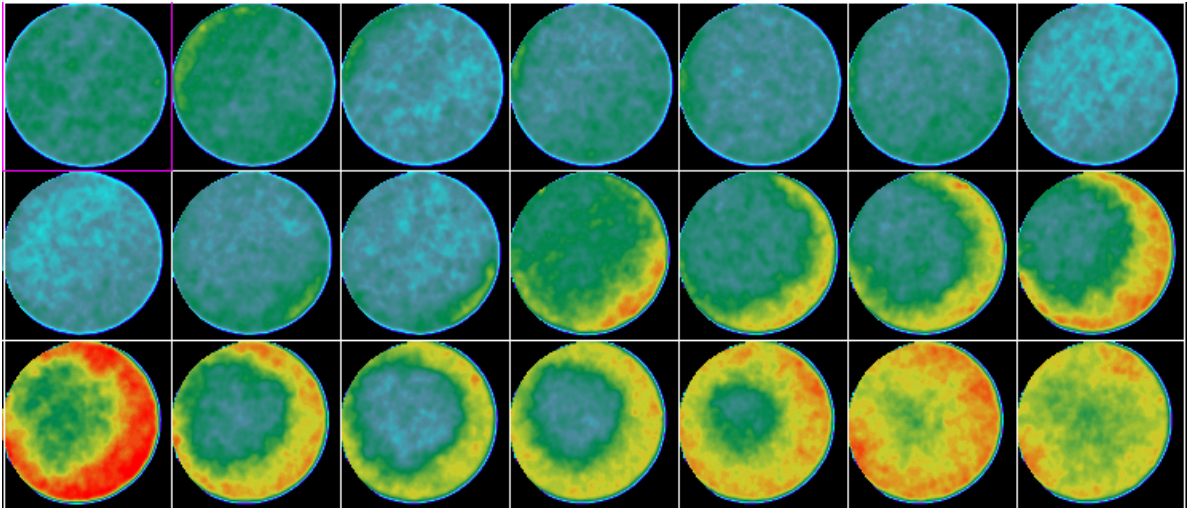


Fig. 1. 9 – CT Scans at 35 minutes after CO₂ injection

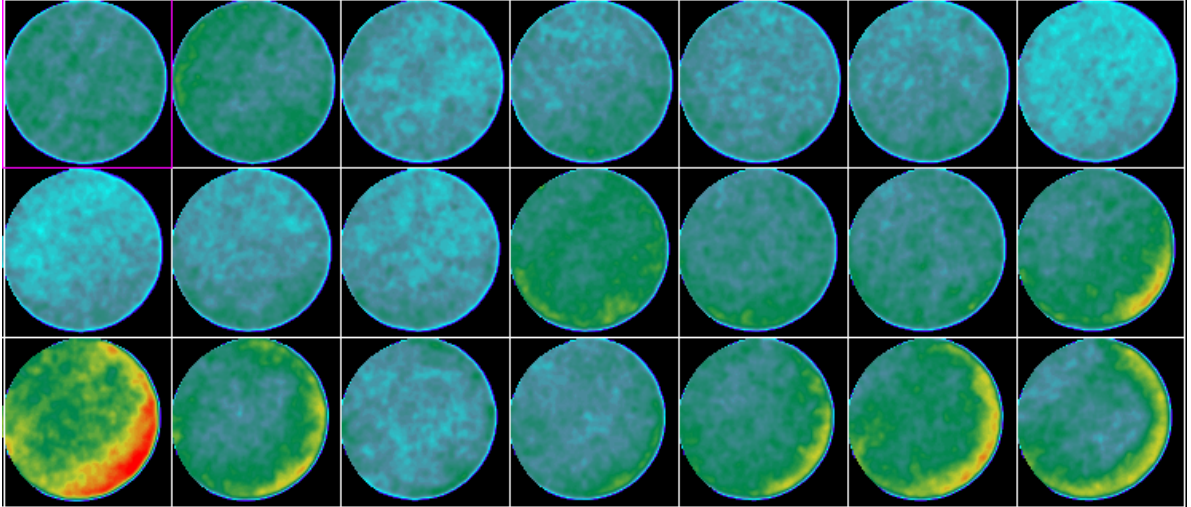


Fig. 1. 10 – CT Scans at 60 minutes after CO₂ injection

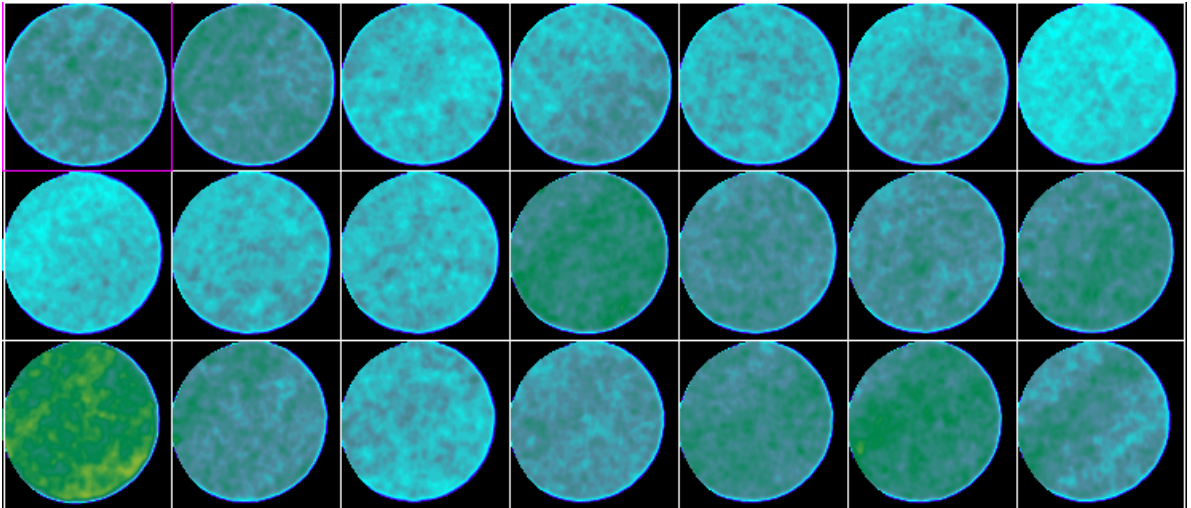


Fig. 1. 11 – CT scans showing almost 100% CO₂ saturated cores at 120 minutes

The above figure (Fig. 1. 11) shows the CT scans at 120 minutes of CO₂ injection. It can be seen that the scans have an almost uniform blue color indicating uniform saturation of CO₂. This was also verified by the fluid recovered at the outlet which was about 99% of the original volume of fluid in the core. The CT image profile plot for CO₂ saturated core is shown in Fig. 1. 15.

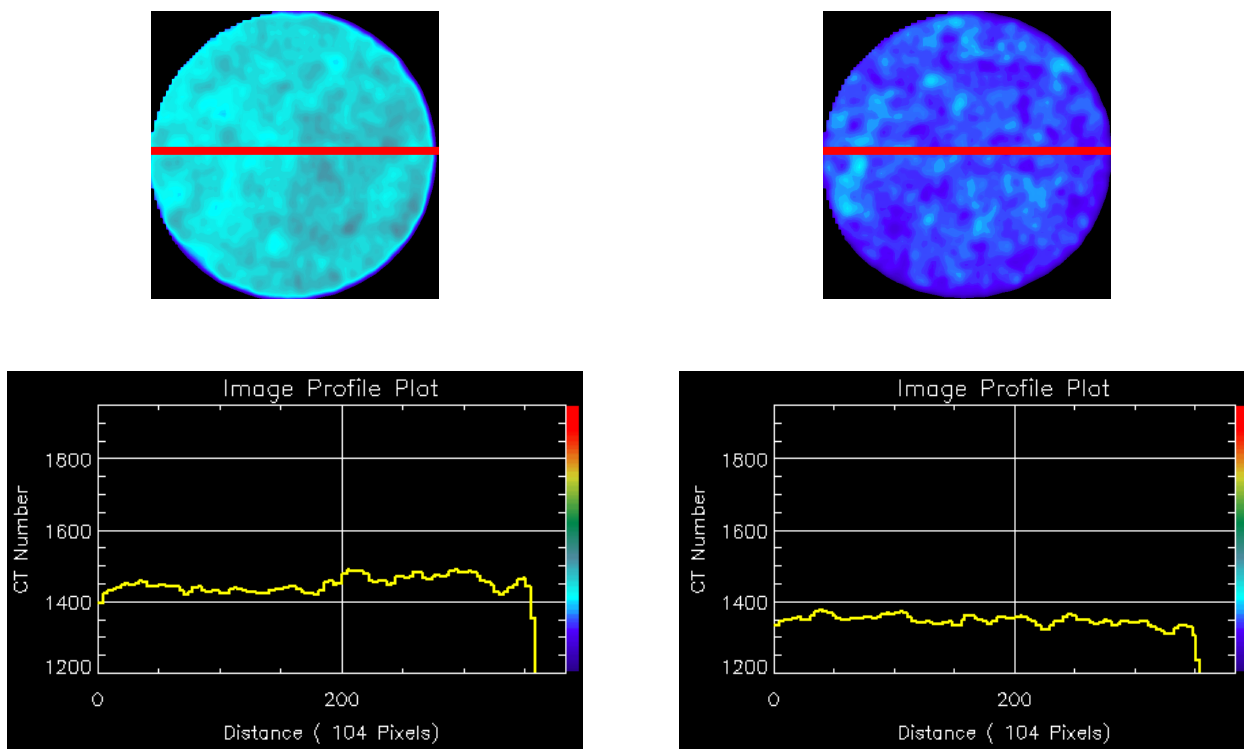


Fig. 1. 12 – CT numbers for dry cores showing a difference of 100 CT numbers for the highest and lowest CT number slices

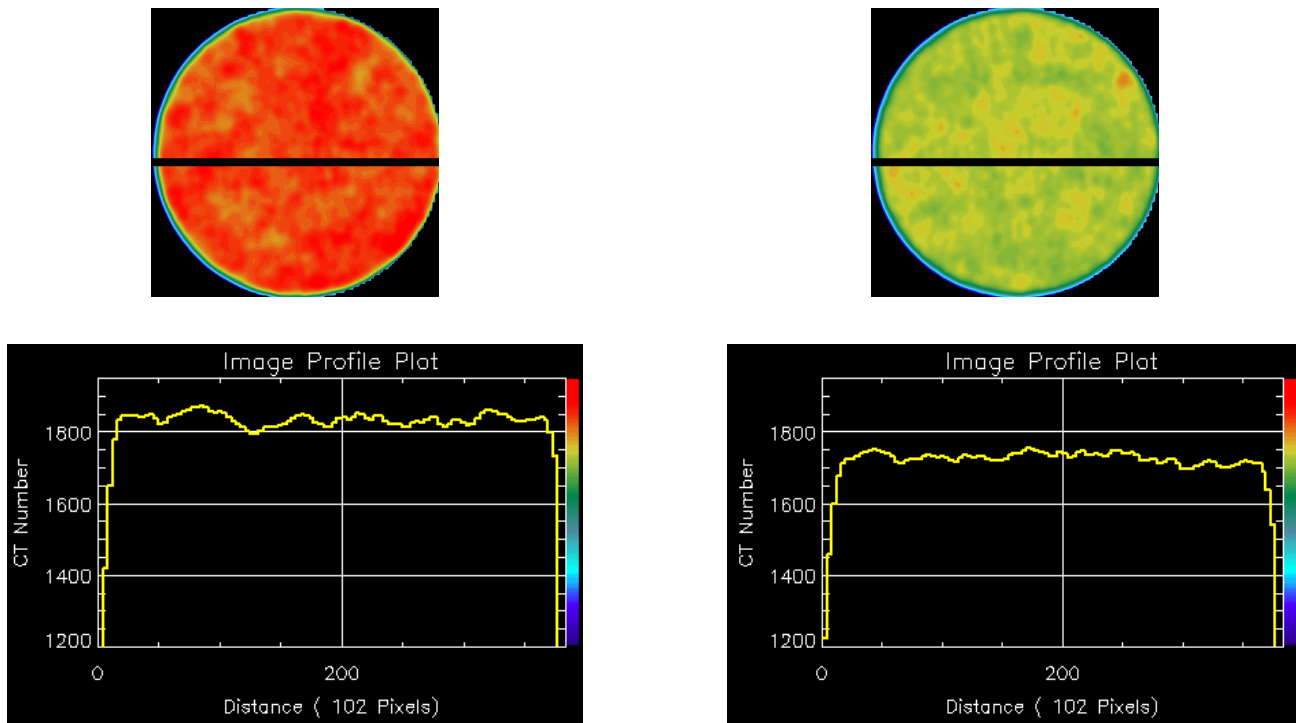


Fig. 1. 13 – CT Numbers for oil saturated core follow same trend as dry core

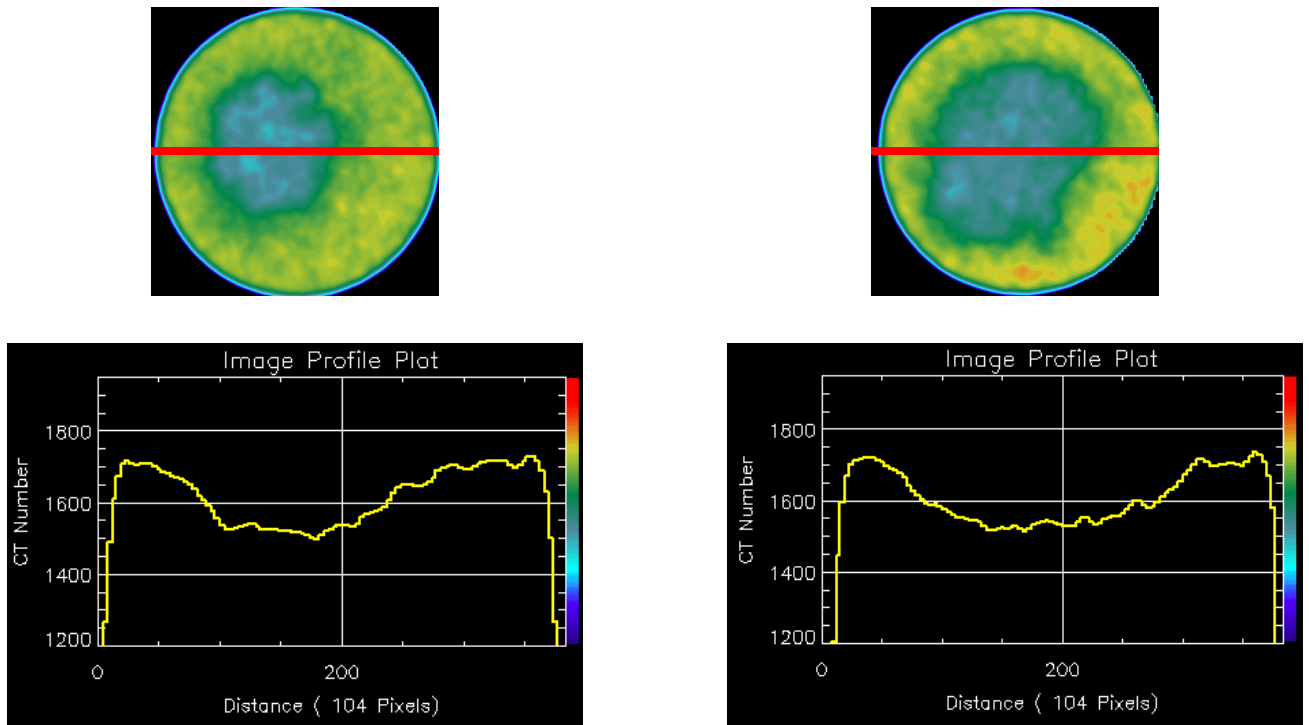


Fig. 1. 14 – Sample plots of CO₂ injected core images showing a decrease in CT number with increase in CO₂ saturation

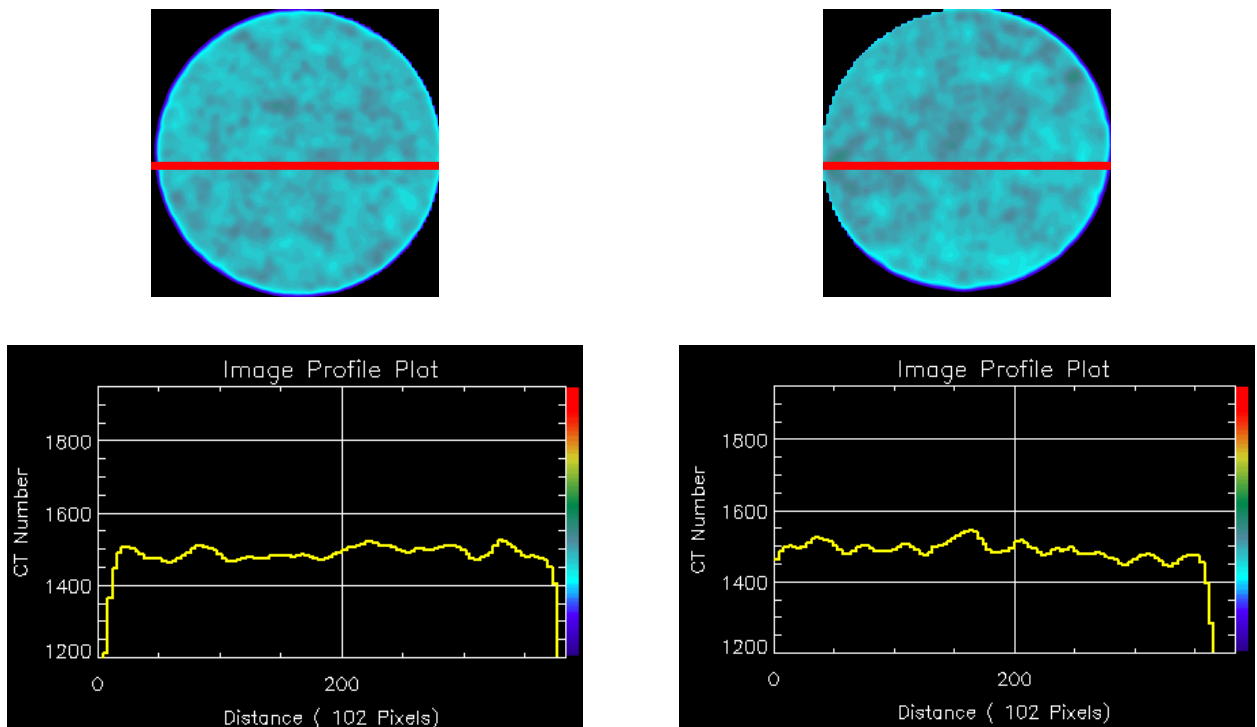


Fig. 1. 15 – CO₂ saturated cores showing uniform CT numbers

A better understanding of the flow of CO₂ in the core can be achieved by seeing the reconstruction of the cross-sectional CT scans during various stages. The reconstructed images are shown in Fig. 1. 16a to 16g.

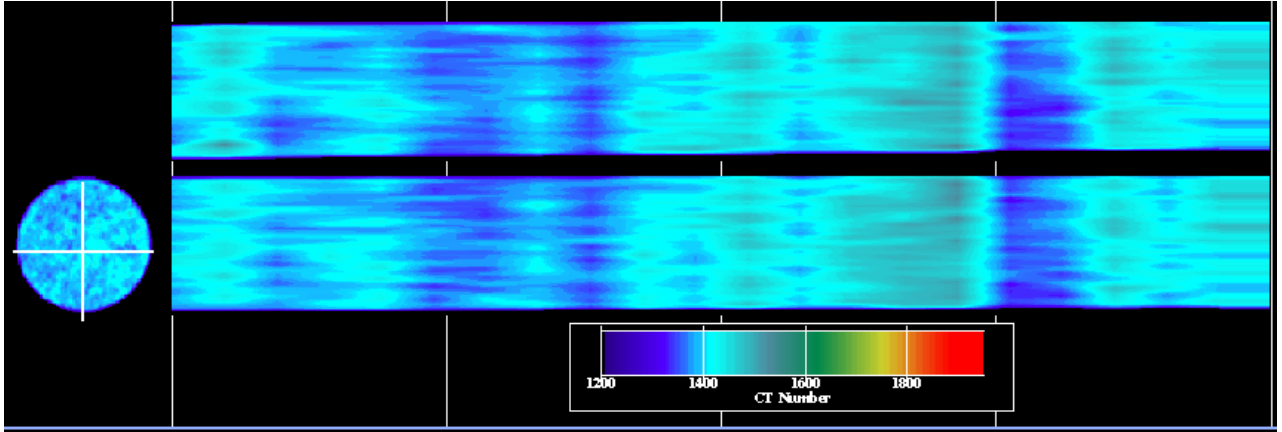


Fig. 1. 16a – Reconstruction of dry core images

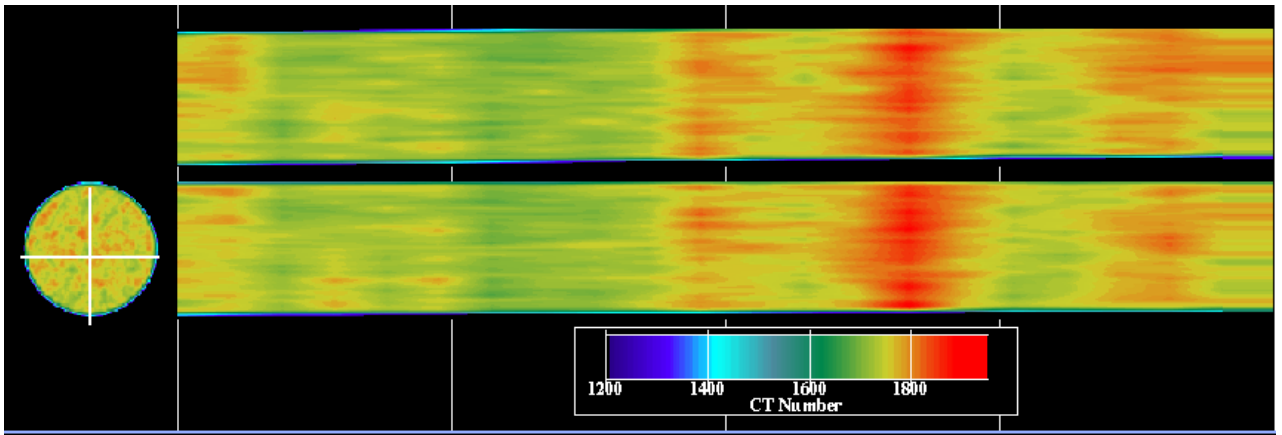


Fig. 1. 16b – Reconstruction of oil saturated core images

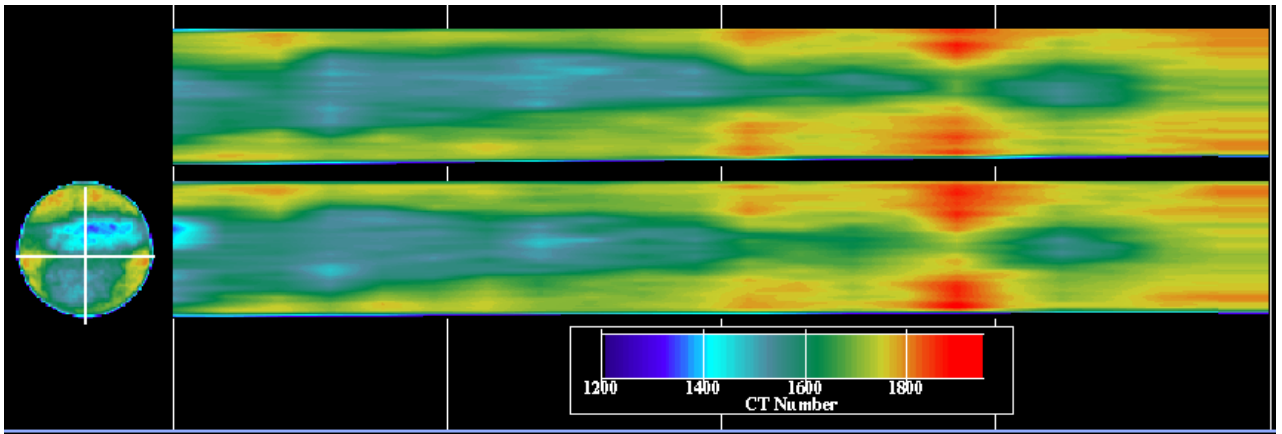


Fig. 1. 16c – CO₂ injection – 15 minutes

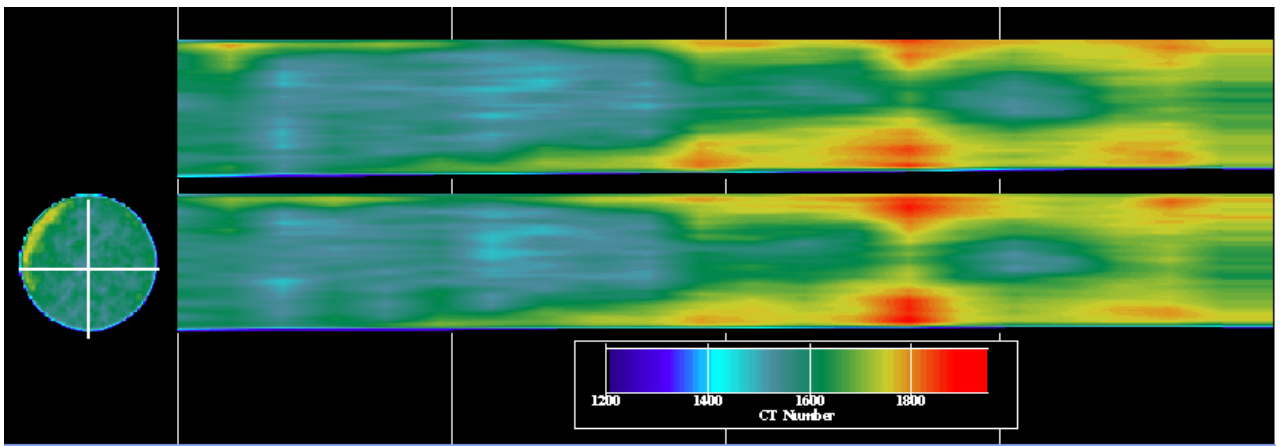


Fig. 1. 16d – CO₂ injection – 25 minutes

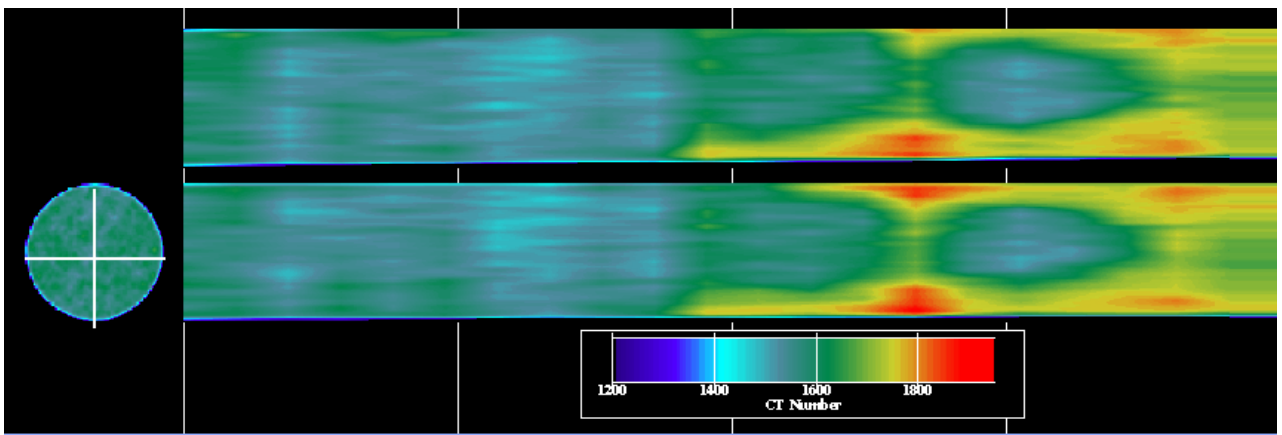


Fig. 1. 16e – CO₂ injection – 35 minutes

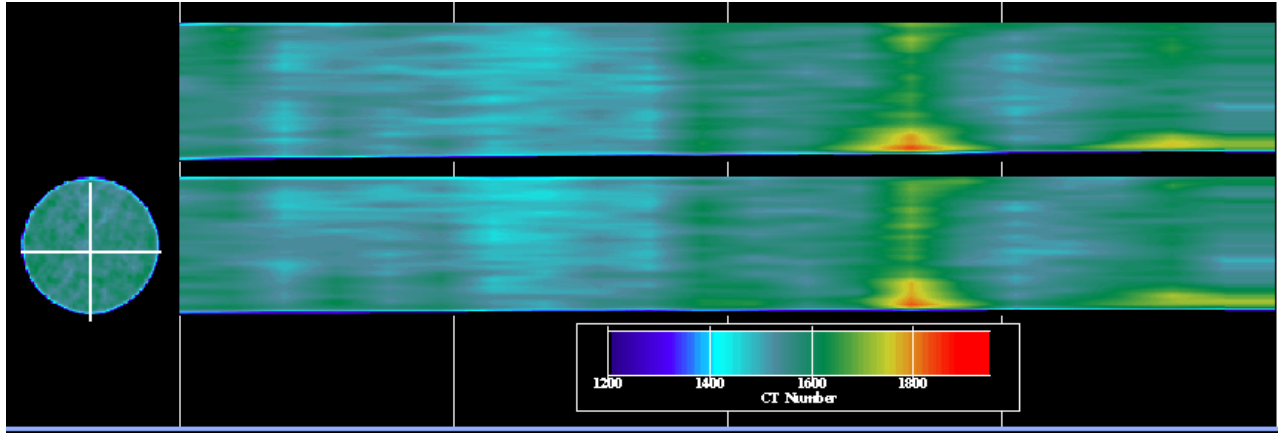


Fig. 1. 16f – CO₂ injection – 60 minutes

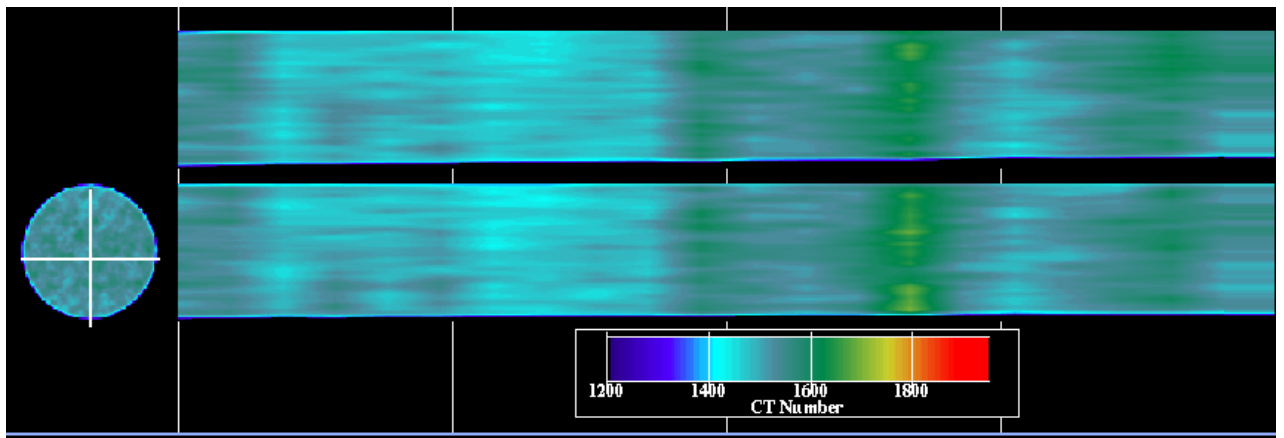


Fig. 1. 16g – CO₂ injection – 120 minutes

The images shown above clearly depict the flow of CO₂ at an injection rate as high as 0.09 cc/min, with the top image showing flow in the horizontal plane and bottom image showing flow in the vertical plane as indicated by the axes in the cross-sectional image. It can be seen that CO₂ enters through the middle of the core and continues to flow that way, bypassing a considerable amount of oil. The path taken by CO₂ shows that the core is a homogeneous one. In a highly heterogeneous core, CO₂ may find a preferential path to breakthrough and continue to flow in that path even after breakthrough, due to the higher trapped gas saturation. But for this core it was seen that injecting CO₂ for a sufficient amount of time allowed CO₂ to contact all regions of the core and recover oil from those regions. The effect of heterogeneity on the flow of CO₂ can be observed by comparing Figs. 16b and 16c. Fig. 1. 16b shows the red colored spots in the second half

of the core that represent regions of higher density and lesser porosity. It can be seen that the CO₂ streak thins down at that particular region and continues to remain like that for some time. This phenomenon was also observed in the cross-sectional images during the different stages. The saturations of CO₂ at different stages during the experiment were also obtained using the CT numbers from the scans. Fig. 1. 17a to 17d show the CO₂ saturation distributions in the core at different times.

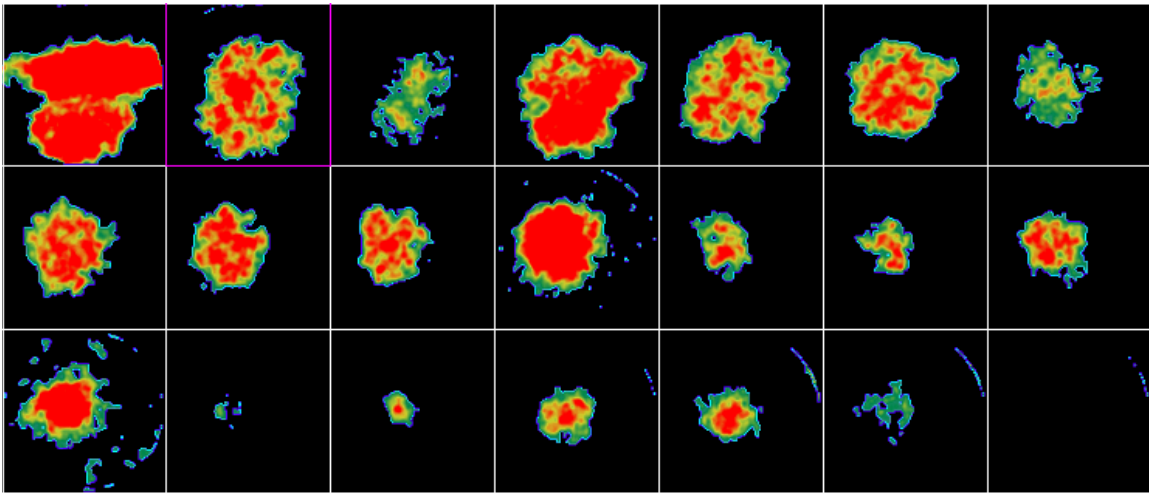


Fig. 1. 17 a. CO₂ saturation distribution at 15 minutes after injection

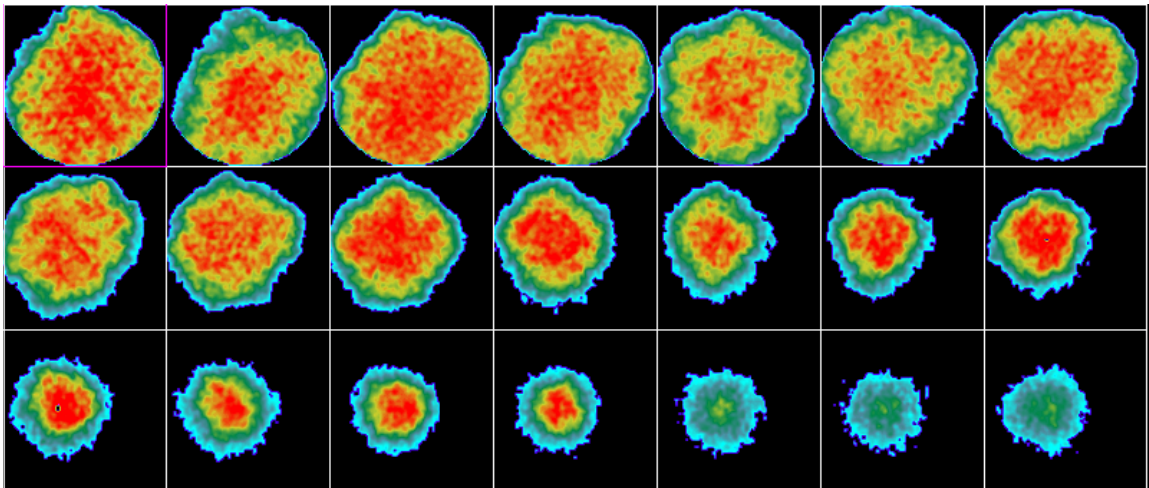


Fig. 1. 17 b. CO₂ saturation distribution at 25 minutes after injection

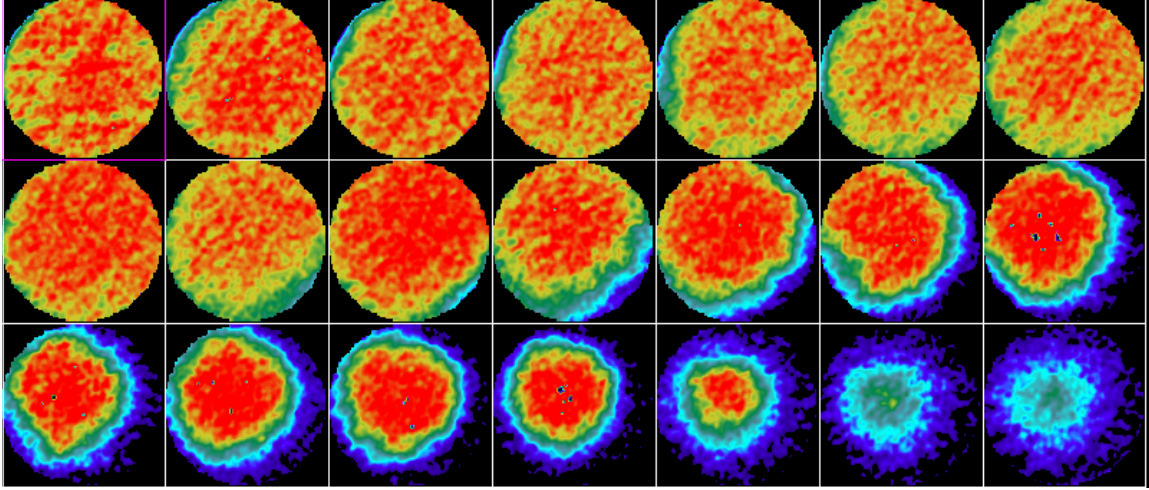


Fig. 1. 17 c. CO₂ saturation distribution at 35 minutes after injection

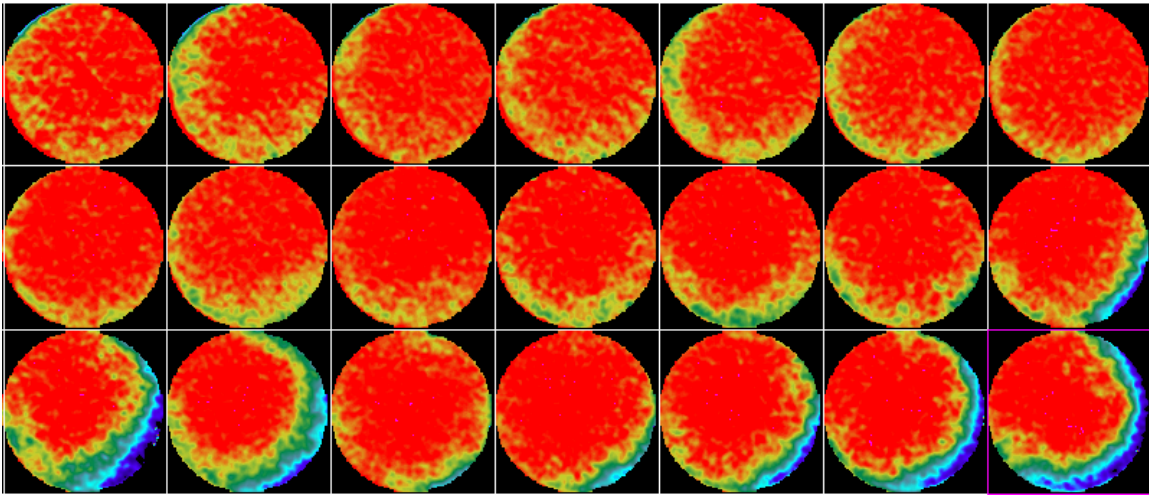


Fig. 1. 17 d. CO₂ saturation distribution at 60 minutes after injection

1.5.2 Low Injection Rate

In this experiment, CO₂ was injected at a rate of 0.01 cc/min. Scans were taken at six different times during the course of the experiment: 30 min, 60 min, 120 min, 150 min, 180 min and 300 min. The last set of scans was taken at a time when the produced fluid was only CO₂. The cross-sectional scans during different stages of the experiment are shown from Figs 18 to 24. Also shown below each scan is the ortho reconstruction of the cross-sectional images.

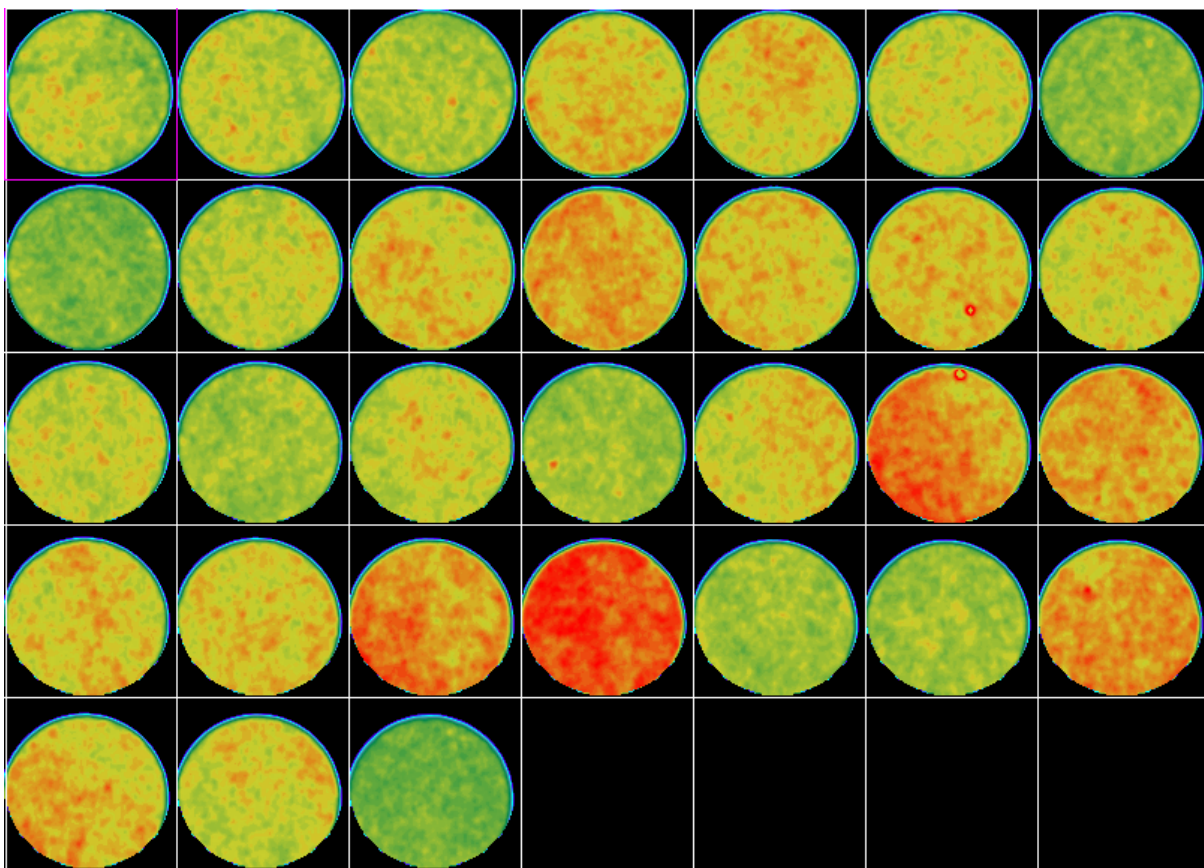


Fig. 1. 18 – Oil saturated core scans

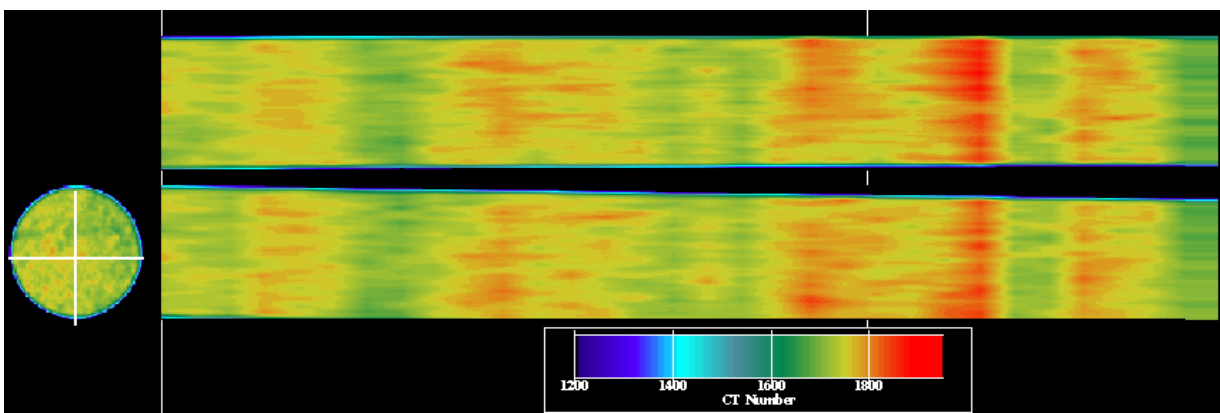


Fig. 1. 18a – Reconstructed image of oil saturated core

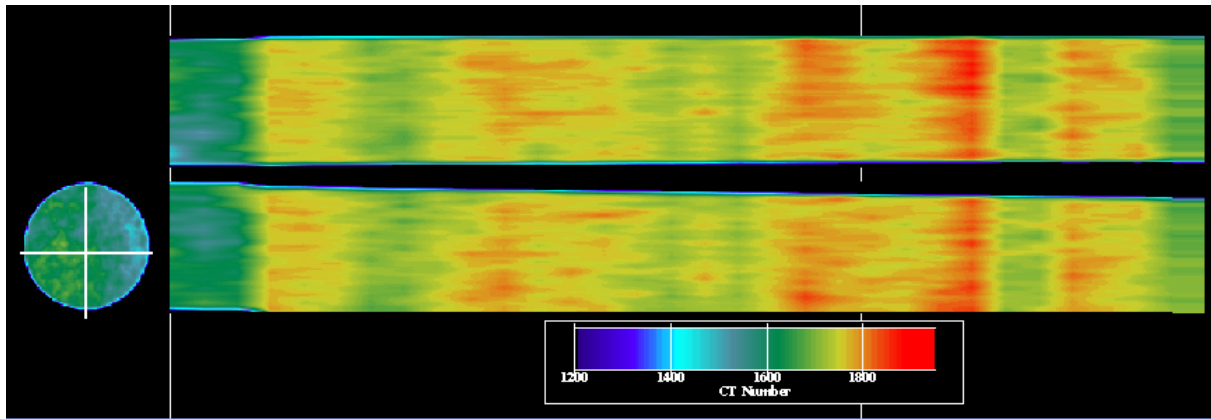


Fig. 1. 19 – CO₂ injection – 30 minutes

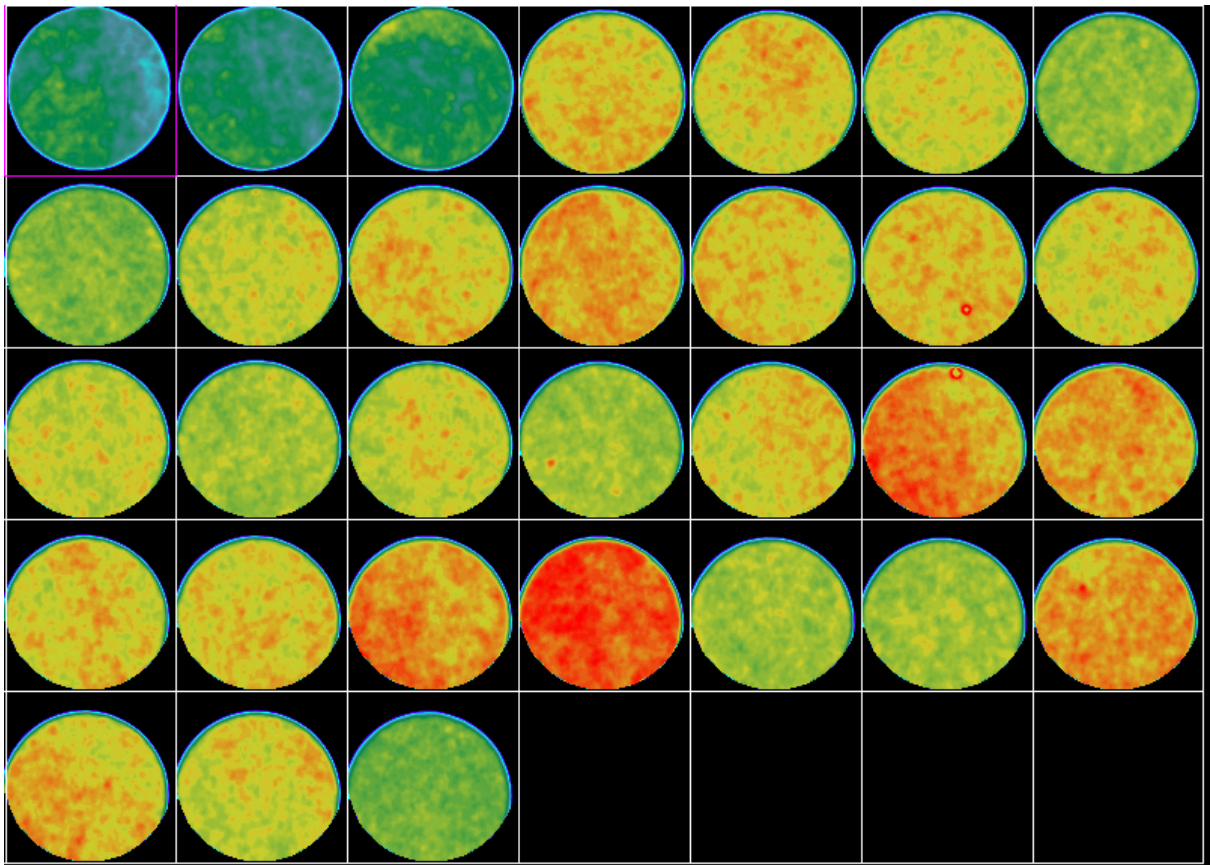


Fig. 1. 19a – Reconstructed image

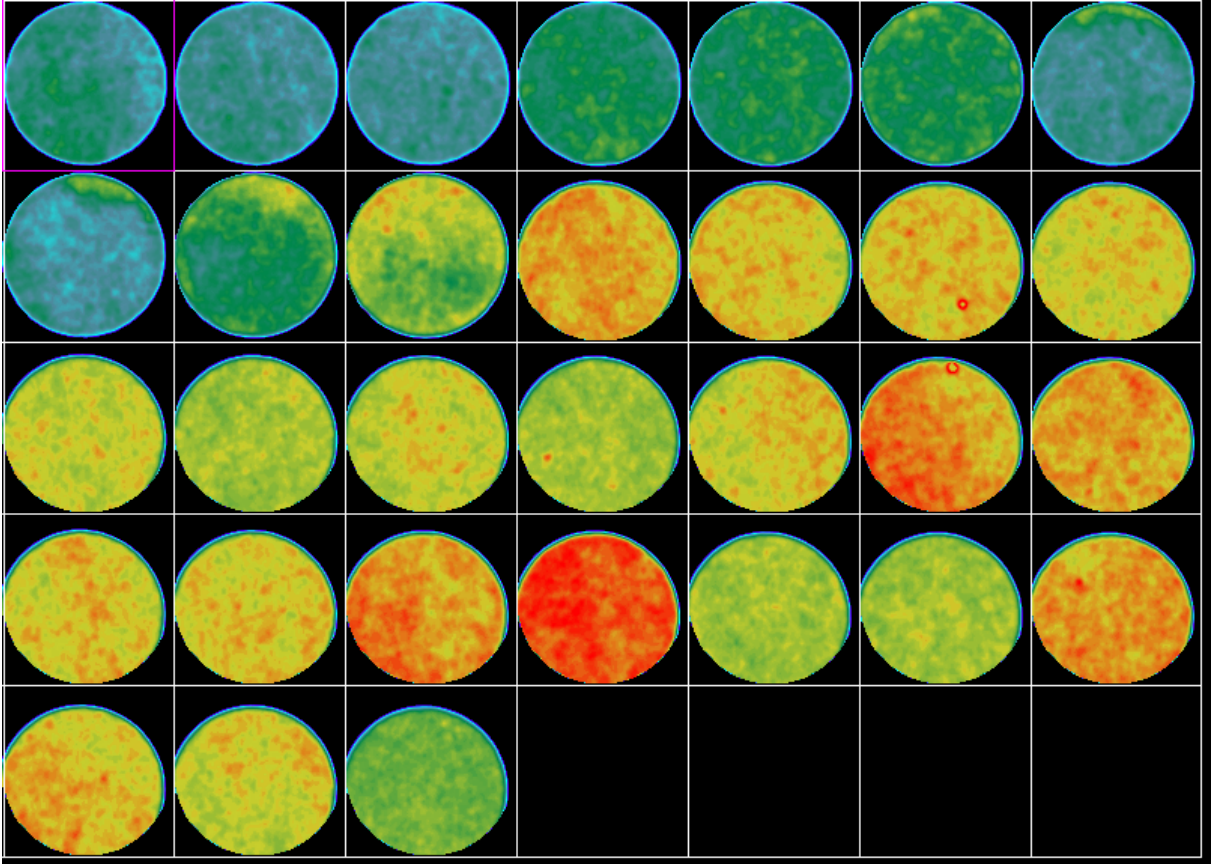


Fig. 1. 20 – CO₂ injection - 60 minutes

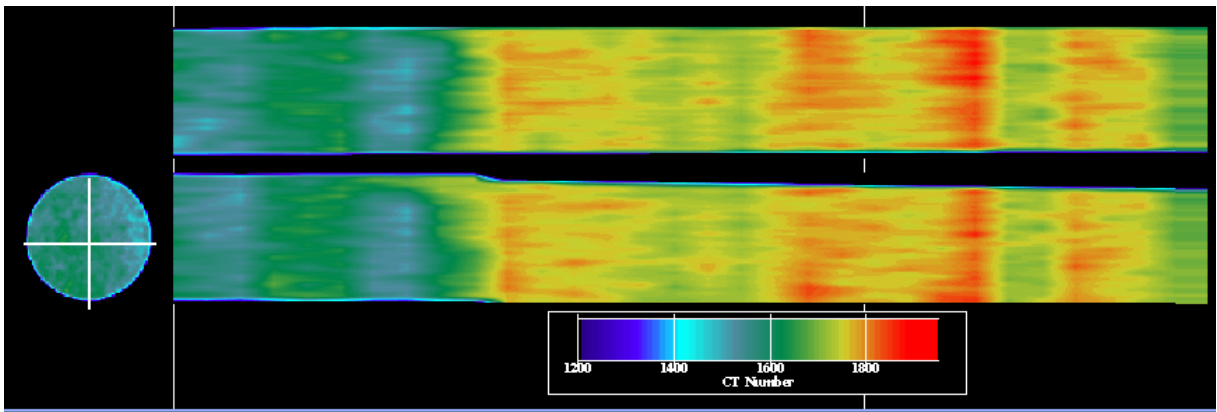


Fig. 1. 20a – Reconstructed image

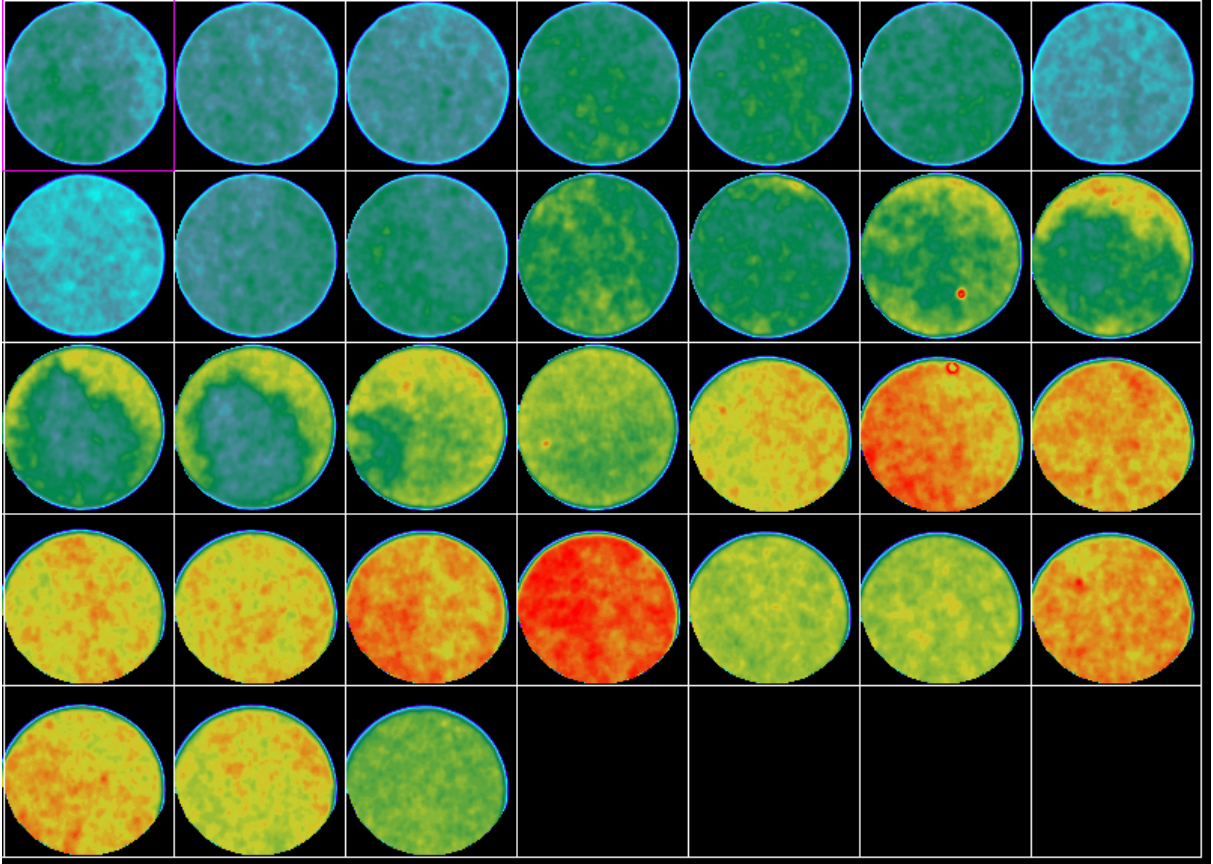


Fig. 1. 21 – CO₂ injection – 120 minutes

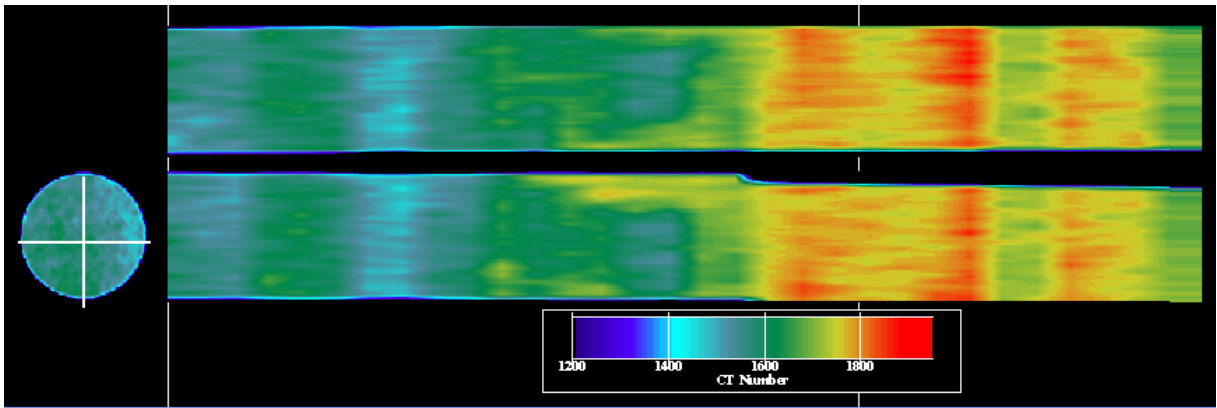


Fig. 1. 21a – Reconstructed image

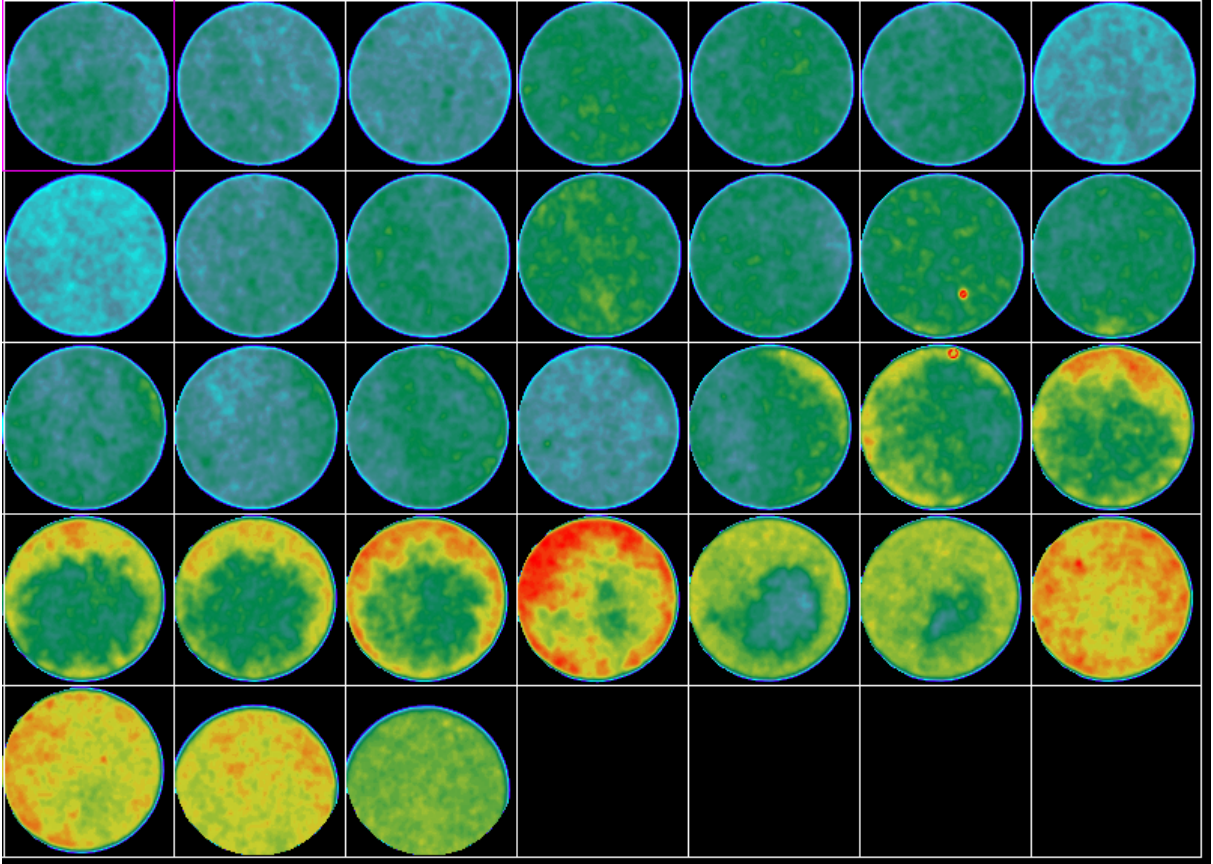


Fig. 1. 22 – CO₂ injection – 150 minutes

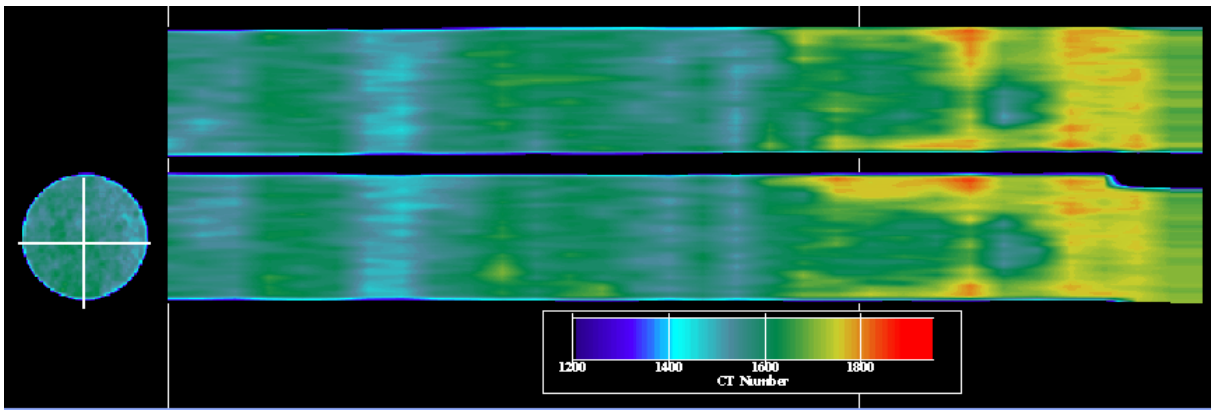


Fig. 1. 22a – Reconstructed image

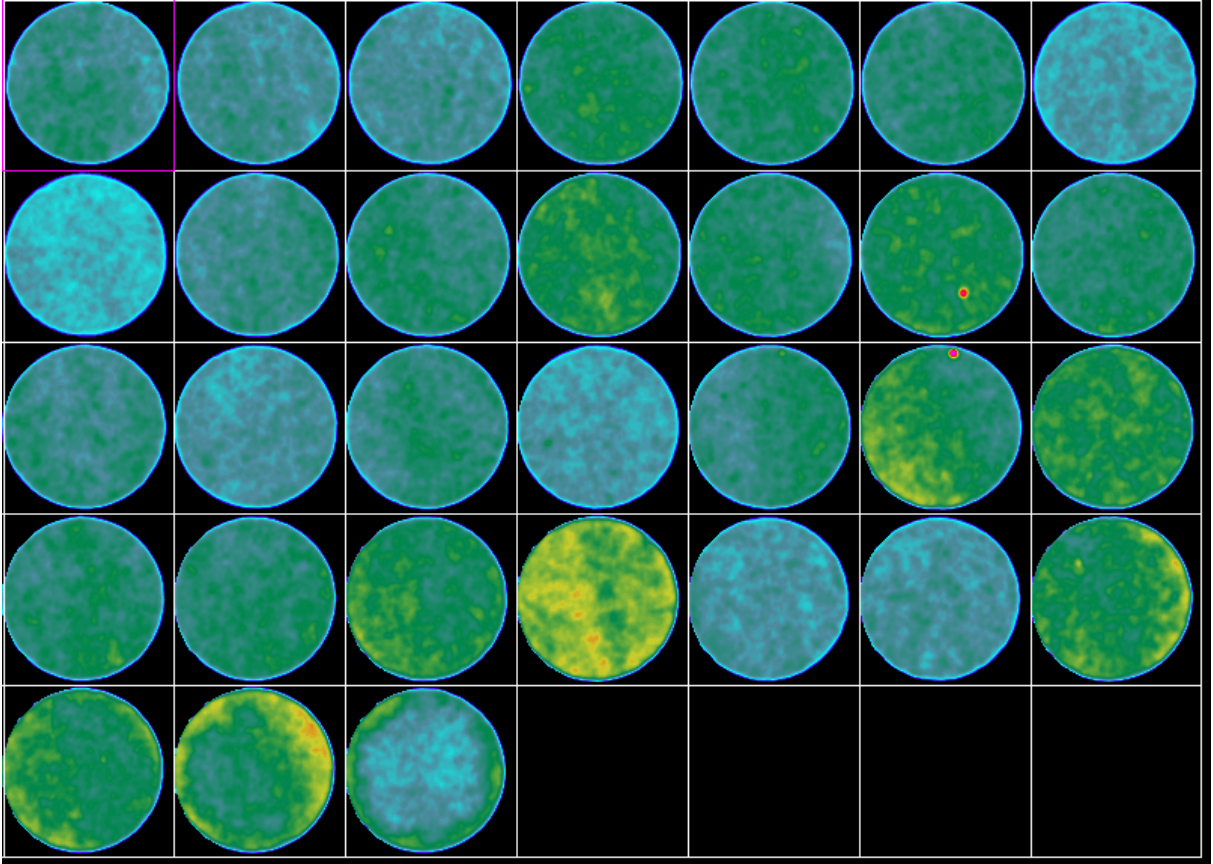


Fig. 1. 23 - CO₂ injection – 180 minutes (CO₂ breakthrough)

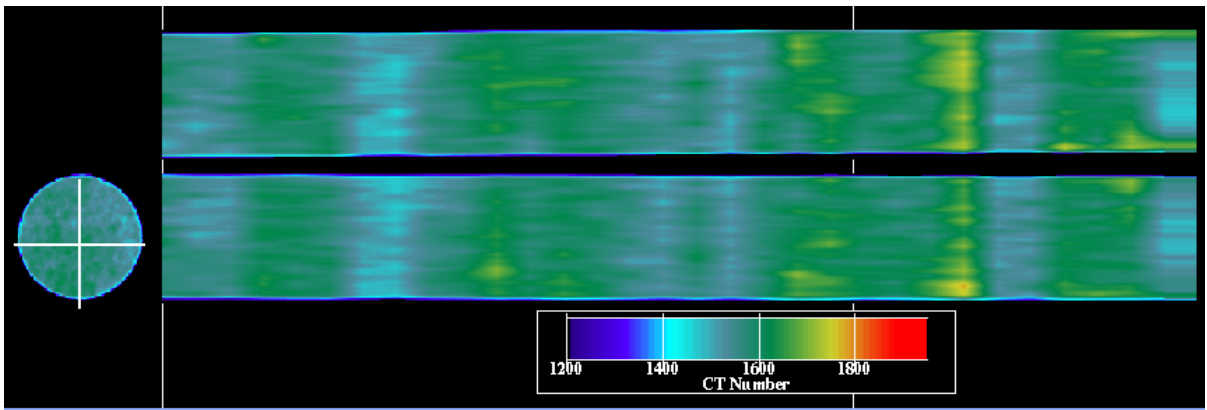


Fig. 1. 23a – Reconstructed image

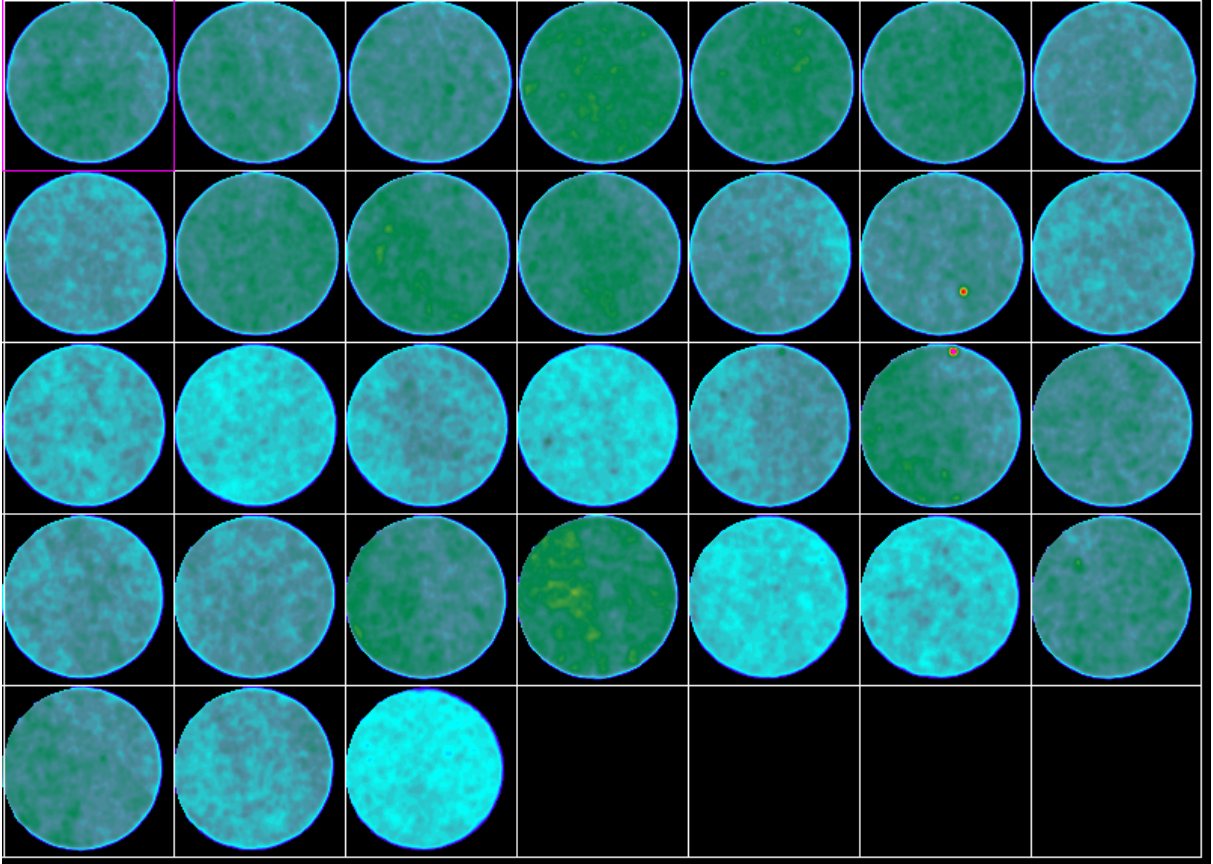


Fig. 1. 24 – Core with 99% CO₂ saturation

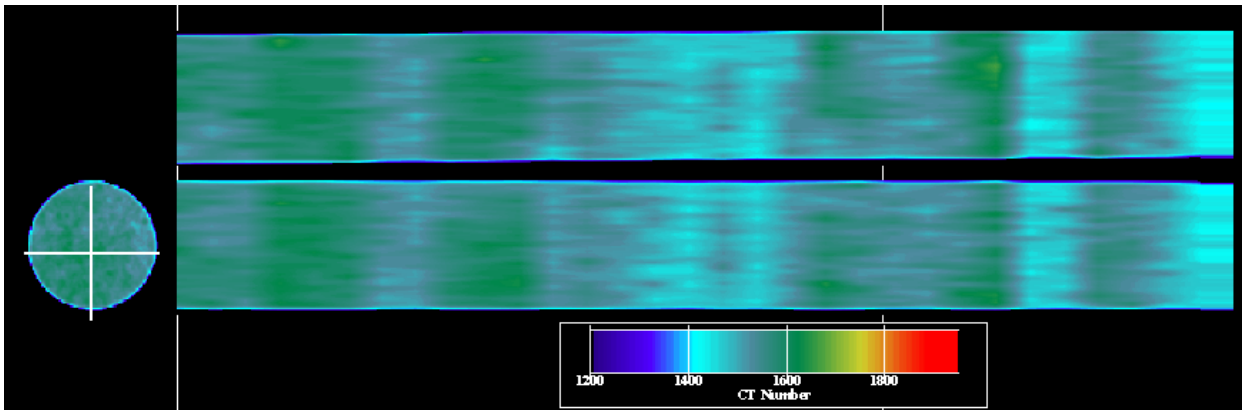


Fig. 1. 24a – Reconstructed image

The above figures clearly depict the effect of injection rate on sweep and utilization of CO₂. It can be seen that at this injection rate, CO₂ does not bypass oil and a very good sweep is obtained. Close observation of the initial reconstructions before breakthrough shows a small oil bank formed at the front. The breakthrough time of CO₂ in this case

reduced drastically compared to the previous case. The effect of heterogeneity in the core is same as that observed in the previous case. Also, the CT numbers observed in this case were in the same range as the previous case and hence the image profile plots have been omitted. The saturations of CO₂ calculated from the scans have been plotted in Figs. 25 and 26.

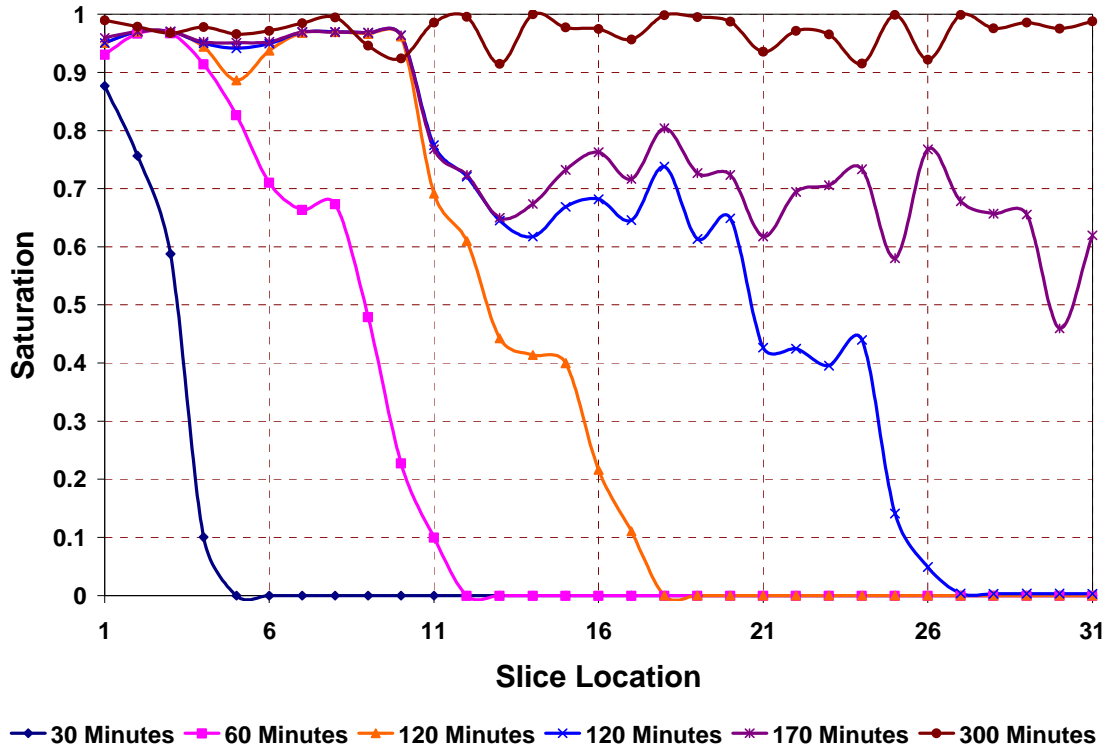


Fig. 1. 25: CO₂ saturations at various slice locations

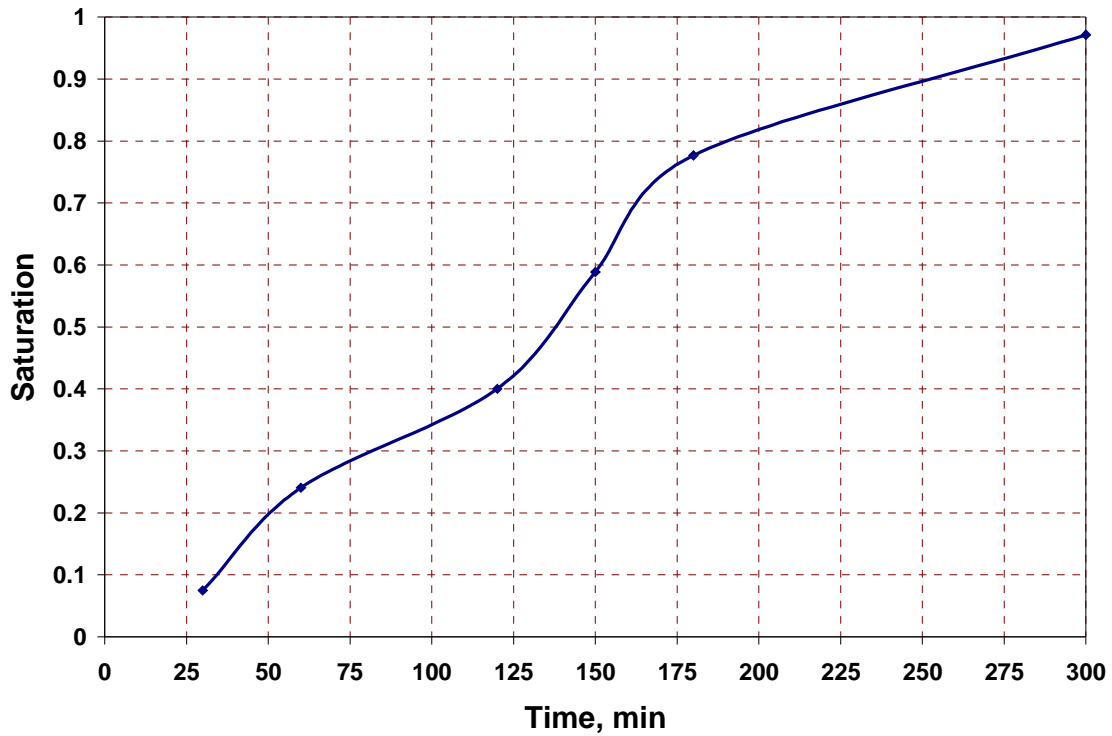


Fig. 1. 26 – Plot of average CO₂ saturation in the core with time

The above figures depict the variation of CO₂ saturation with distance along the length of the core and the average CO₂ saturation during different times. Fig. 1. 24 shows that the saturation at different locations increases with time, though with minor fluctuations due to numerical approximations by the software. Fig. 1. 25 shows the average CO₂ saturation in the core during various stages of injection. The final saturation shown is about 97.5% while the actual recovery was about 99%. This is acceptable since the error is less than 1%.

1.5.3 Fractured Core

In this experiment, the core was fractured prior to injecting CO₂. The CT scan images for the fractured core are shown in Fig. 1. 27.

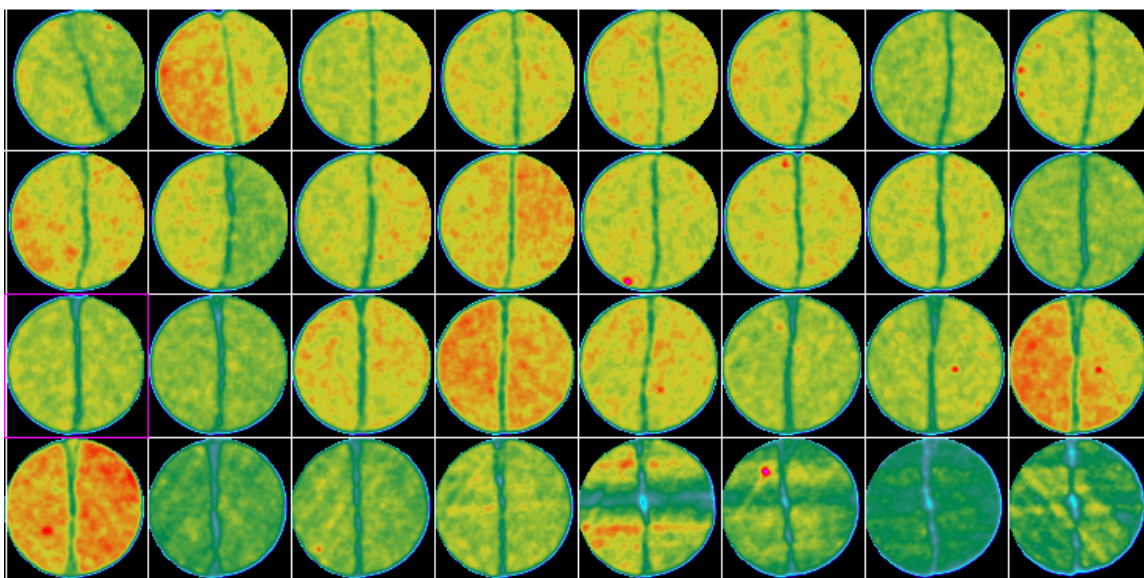


Fig. 1. 27 – CT scan images of oil saturated, fractured core

It can be seen from the images that the fracture has a dark green color. This is a region with lower CT number. The image profile plot for two sample cross-sections is shown below (Fig. 1. 28).

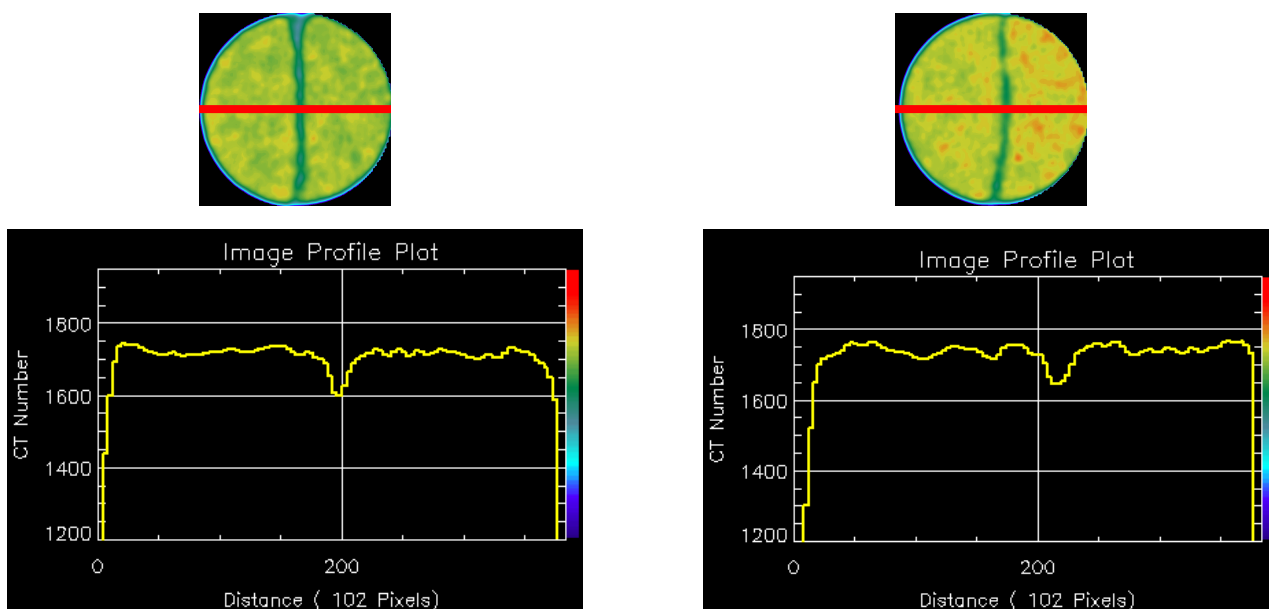


Fig. 1. 28 – CT image profile plot for a fractured core

The above scan of the oil saturated fractured core was taken with a certain level of backpressure to ensure that the fracture was filled with oil. Now, since the fracture is filled with oil, one would expect the CT number at the fracture to go down to 800, which is the CT number for doped oil. But this does not happen as the CT number at the fracture is influenced by the core material surrounding it, a condition termed “multi sampling”. Thus it can be seen that while the Ct number of the matrix is about 1750, the CT number at the fracture does not go all the way down to 800, but stays at about 1600. A less dense fluid at the fracture would reduce the CT number even more, but the actual CT number of the fluid can never be achieved. Shown below are the cross-sectional images of the core after CO₂ injection was started (Fig. 1. 29).

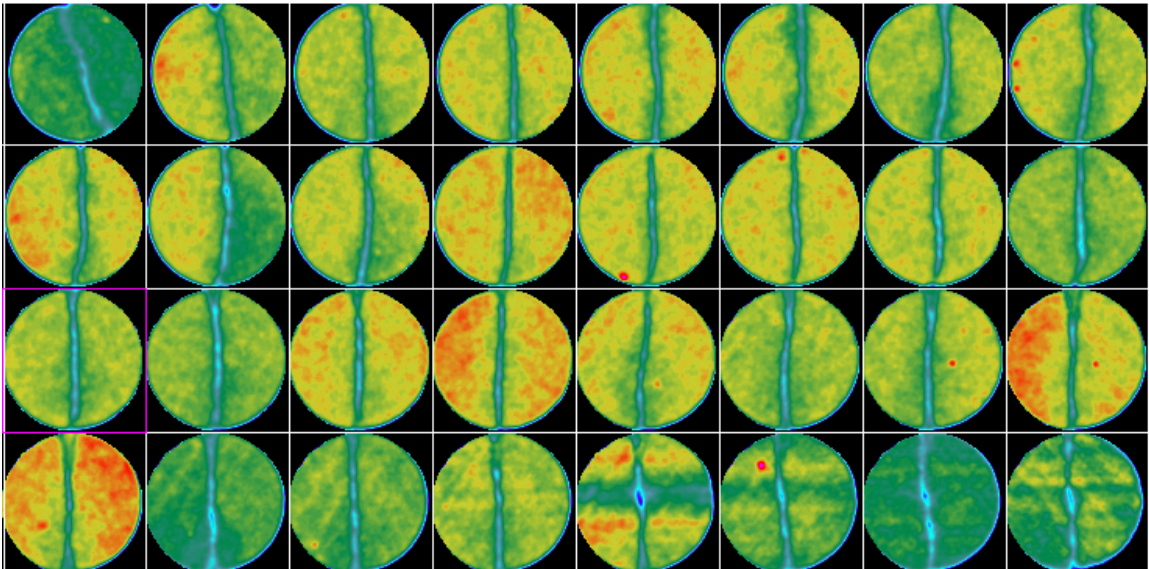


Fig. 1. 29 – CT scan images during CO₂ injection

Also shown is the CT image profile plot for the above scans (Fig. 1. 31). It can be seen from the image profile plot the CT number at the fracture drops to about 1450, indicating that CO₂ is flowing through the fracture. The main observation during this experiment was the path taken by CO₂ through the core. It can be seen from the above figure that only a very all the CO₂ flows through the fracture and only a very small amount has entered the matrix. Very early breakthrough of CO₂ was observed (about 7 minutes after start of injection) even at a low injection rate of 0.03 cc/min. This indicates that the injection rate has to be reduced even further to prevent early breakthrough and allow

entry of CO₂ into the matrix to improve recovery. Fig. 1. 31 and 32 show the ortho reconstructions of the cross sectional scans.

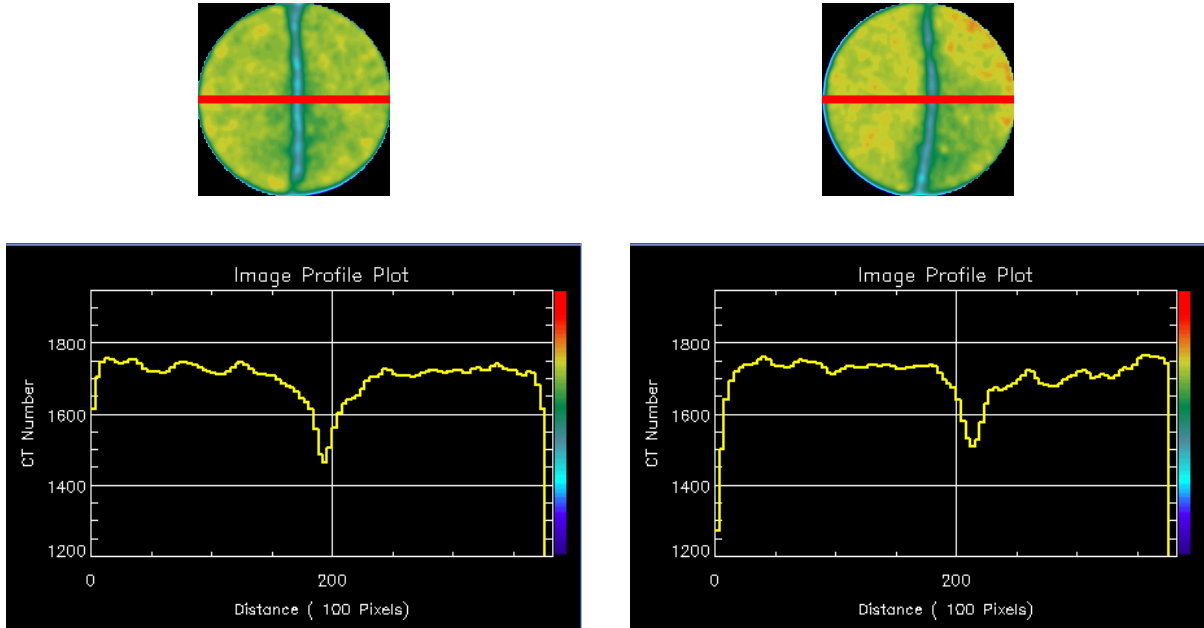


Fig. 1. 30 – CT image profile plots during CO₂ injection

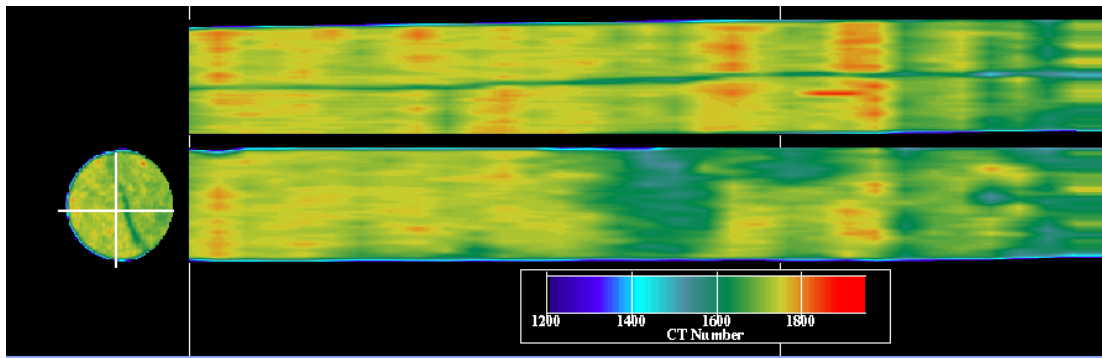


Fig. 1. 31 – Ortho reconstruction of oil saturated fractured core

The above image shows the reconstruction of the cross sectional scans in two planes. The top image is perpendicular to the fracture plane and shows the entire length of the fracture. The bottom image should show one of the fracture faces. But as can be seen from the cross-section at the left, the bottom image includes only a part of the fracture as indicated by the white vertical line cutting the fracture at only a few points. This is because the fracture does not lie in one single plane. For the same reason, the fluid is not

completely seen in the fracture plane. To overcome this problem, Fig. 1.32 was reconstructed using two different planes, one containing the first half of the fracture and the other containing the second half of the fracture. The flow of CO₂ through the fracture is now clearly seen.

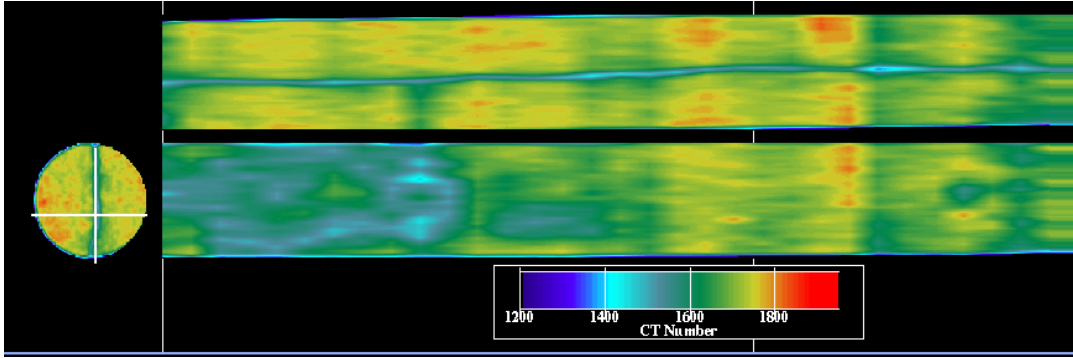


Fig. 1. 32a – Reconstruction including the first half of the fracture shows CO₂ flow (blue color)

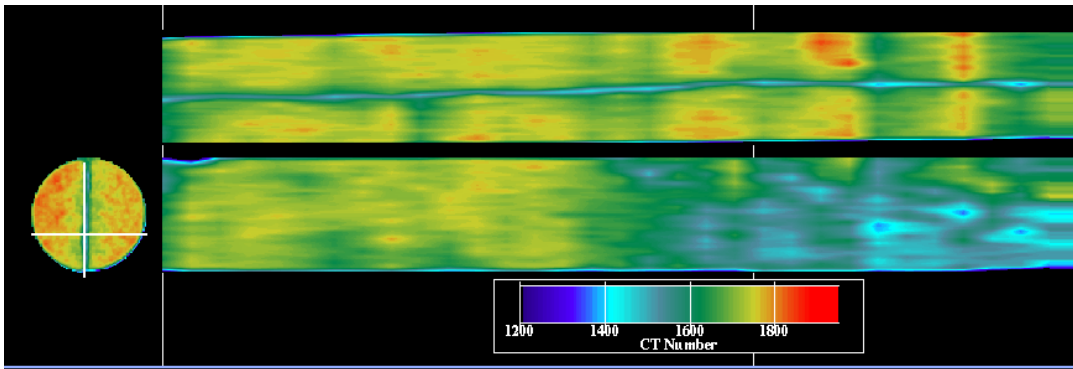


Fig. 1. 32b – Reconstruction including the second half of the fracture face with CO₂

1.6 Conclusions

1. Injection rate plays an important role in affecting oil recovery and breakthrough.
2. Early breakthrough and higher oil bypass are observed at high injection rates.
3. Low injection rate gives better sweep and higher recovery, but this is not attractive as the recovery is too slow
4. In a fractured system, fluid flow occurs mainly through the fractures and a considerable amount of time is required for the injection fluid to penetrate the matrix.
5. An alternative method like WAG is necessary to reduce the mobility of CO₂ in the fractured system.

1.7 References

1. Martin, D.F. and Taber, J.J.: "Carbon Dioxide Flooding," *JPT* (April 1992) 394-400.
2. Yaghoobi, H. *et al.*: "Improving CO₂ Floods in Heterogeneous Media," paper SPE 35403 presented at the 1996 SPE/DOE Tenth Symposium on Improved Oil Recovery, Tulsa, OK, 21-24 April.
3. Uleberg, K. and Hoier, L.: "Miscible Gas Injection in Fractured Reservoirs," paper SPE 75136 presented at the 2002 SPE/DOE Tenth Symposium on Improved Oil Recovery, Tulsa, OK, 13-17 April.
4. Holm, L.W. and O'Brien, L.J.: "Factors to Consider When Deciding a CO₂ Flood," paper SPE 14105 presented at the 1986 International Meeting on Petroleum Engineering held at Beijing, China, March 17-20.
5. Mungan, N.: "An Evaluation of CO₂ Flooding," paper SPE 21672 presented at the 1991 SPE Western Regional Meeting held at Long Beach, CA, March 20-22.
6. Bergosh, J. L., Marks, T. R. and Mitkus, A. F.: "New Core Analysis Techniques for Naturally Fractured Reservoirs," paper SPE 13653 presented at the 1985 Annual California Regional Meeting, Bakersfield, March 27-29.
7. Honarpour, M. M., Cromwell, V., Hatton, D. and Satchwell, R.: "Reservoir Rock Descriptions Using Computed Tomography (CT)," paper SPE 14272 presented at the 1985 Annual Technical Conference and Exhibition, Las Vegas, Sept. 22-25.

8. Honarpour, M. M., McGee, K. R., Crocker, M. E., Maerefat, N. L. and Sharma, B.: "Detailed Core Description of a Dolomite Sample from the Upper Madison Limestone Group," paper SPE 15174 presented at the 1986 Rocky Mountain Regional Meeting, Billings, May 19-21.
9. Narayanan, K. and Deans, H. A.: "A Flow Model Based on the Structure of Heterogeneous Porous Media," paper SPE 18328 presented at the 1988 Annual Technical Conference and Exhibition, Houston, Oct. 2-5.
10. Jasti, J., Jesion, G. and Feldkamp, L.: "Microscopic Imaging of Porous Media Using X-Ray Computer Tomography," presented SPE 20495 at the 1990 Annual Technical Conference and Exhibition, New Orleans, Sept. 23-26.
11. Hidajat, I. *et al.*: "Study of Vuggy Carbonates using X-Ray CT Scanner and NMR," paper SPE 77396 presented at the 2002 SPE Annual Technical Conference and Exhibition, San Antonio, Texas, 29 September - 2 October .
12. MacAllister, D. J., Miller, K. C., Graham, S. K. and Yang, C-T.: "Application of X-Ray CT Scanning to the Determination of Gas-Water Relative Permeabilities," paper SPE 20494 presented at the 1990 Annual Technical Conference and Exhibition, New Orleans, Sept. 23-26.
13. Withjack, E. M.: "Computed Tomography for Rock-Property Determination and Fluid-Flow Visualization," paper SPE 16951 presented at the 1987 SPE Annual Technical Conference and Exhibition, Dallas, Texas, September 27-30.
14. Wellington, S. L and Vinegar, H. J: "X-Ray Computed Tomography," paper SPE 16983.
15. Hicks Jr., P.J. *et al.*: "An Experimental Study of Miscible Displacements in heterogeneous Carbonate Cores Using X-Ray CT," paper SPE 20492.
16. Wellington, S. L. and Vinegar, H. J.: "CT Studies of Surfactant- Induced CO₂ Mobility Control," paper SPE 14393 presented at the 1985 SPE Annual Technical Conference and Exhibition, Las Vegas, September 22-25.
17. Yamamoto, J. *et al.*: "An Analysis of CO₂ WAG Coreflood by Use of X-Ray CT," paper SPE 38068 presented at the 1997 SPE Asia Pacific Oil and Gas Conference, Kuala Lumpur, Malaysia, April 14-16.

18. Oshita, T. *et al*: “Early Water Breakthrough – X-Ray CT Visualizes How it Happens in Oil-Wet Cores,” paper SPE 59246 presented at the 2000 SPE Asia Pacific Conference on Integrated Modeling for Asset Management, Yokohama, Japan, 25-26 April.
19. Alajmi, A.F. and Grader, A.S.: “Analysis of Fracture-Matrix Fluid Flow Interactions Using X-Ray CT,” paper SPE 65628 presented at the 2000 Eastern Regional Meeting, Morgantown, West Virginia, Oct. 17-19.
20. Holm L.W., Josendal, V.A.: “Mechanisms of Oil Displacement by Carbon Dioxide,” paper SPE 4736.
21. Holm, W.: “Evolution of the Carbon Dioxide Flooding Process,” *JPT* (November 1987), 1337-1342.

Chapter II

Possible Strategies to Mitigate CO₂ Flooding Bypassing Mechanisms in Fracture-Dominated Reservoirs

2.1 Introduction

Fractured reservoirs form a large percentage of the world's hydrocarbon reserves. However, in spite of their wide occurrence and huge reserves, the oil recovery from most of these reservoirs is extremely low. This can be attributed to their poor response to both secondary and tertiary recovery operations. In a fractured system, the displacement process is dependent on the fracture-matrix geometry, size and interaction apart from other physical phenomena ⁽¹⁾. Uleberg and Hoier ⁽²⁾ suggest that the injection fluid tends to flow through the highly permeable fractures, often resulting in early breakthrough and poor sweep efficiency. This is especially true when the displacing phase is a highly mobile fluid like CO₂. In order to improve the sweep efficiency and delay breakthrough, the mobility of the displacing fluid in fractures, has to be controlled.

Several field cases ⁽³⁾⁽⁴⁾⁽⁵⁾⁽⁶⁾ and laboratory experiments ⁽⁷⁾⁽⁸⁾⁽⁹⁾ indicate that the water-alternating-gas (WAG) process has been an effective mobility control method in most cases. In a fairly homogeneous system, water invades the zones previously invaded by the gas, subsequently diverting the gas into other zones ⁽¹⁰⁾. But a completely different situation prevails in the presence of extreme heterogeneities like fractures. In such a case, the conformance control agent must be able to effectively divert the fluid into the matrix, thereby delaying breakthrough and reducing oil bypass. But the performance of WAG in terms of mobility control in fractures has not been adequately studied.

The goal of this work is to investigate CO₂ flow in fractures, in the presence of water as a mobility control agent. Immiscible CO₂ flooding experiments were first conducted using homogeneous cores (in the absence of fracture) at different injection rates to serve as a comparison for the fractured core experiments. The cores were then fractured using a core splitter. Experiments were then conducted in fractured cores with continuous CO₂ injection and injection of specific pore volumes of water and CO₂. One experiment was also performed after adding a cross-linker to the solution to form a gel. During each

injection, CT scans covering the entire length of the core were taken in order to study fluid transport in the matrix and the fracture. Saturation distributions were obtained at various stages during the course of the experiment.

2.2 Experimental Setup

The experimental setup consists of five main components – the injection system, the coreflood cell, HD 200 X-Ray CT scanner, the production system and the data acquisition system. A brief description of each of the components is given below.

The injection system consists of two sets of one-liter accumulators one each for the oil and water and one two-liter accumulator for CO₂. All the accumulators are connected to an ISCO 5000 D syringe pump. The pump is equipped with a programmable controller, which it can be set to deliver at a constant flow rate or a constant pressure. Water is injected below the piston in the accumulator and this increases the pressure of the fluid above the piston to the desired level. A flow-switching valve is used to inject oil, water or CO₂ into the coreflood cell.

The core holder measuring 21 in. long is made up of aluminum for use with the CT scanner. It is capable of holding cores up to 1 ft. in length and 1 in. in diameter. A viton Hassler sleeve that surrounds the core is secured to plungers at the ends of the core holder. The coreflood cell has an inlet for hydraulic oil that is used to apply overburden pressure. A pump is used to pressurize the cell by injecting hydraulic oil into the Hassler sleeve – inner wall annulus and pressures up to 7000 psi can be obtained in this manner.

The X-Ray CT scanner is a fourth generation Universal systems HD 200 system with a resolution of 0.3 mm x 0.3 mm. This scanner can be used to scan a maximum diameter of 48 cm with a maximum scan time of 4 sec per scan. Cross sectional scans of the core sample are made at regular intervals during the experiment. The data obtained from the CT scanner is transferred to the image processing system installed in a Sun workstation. The cross sectional images can then be used for porosity and saturation determination or reconstructed for flow visualization.

The outlet end of the core holder is connected to a precision needle valve, which serves as the backpressure regulator, and is used to increase pressure in the system. Also connected is a high precision metering valve to allow minute adjustments to the fluid flow

rate. The produced fluid is collected in a graduated cylinder and any gas produced is measured using a wet test meter.

Two Omega pressure transducers one each at the inlet and the outlet are used in conjunction with an Omega OMB 55 data acquisition system. The pressures can be observed and acquired real time from the personal computer connected to the DAQ.

A schematic of the experimental setup is shown in Fig. 2.1.

2.3 Experimental Procedure

The oil used for the experiments is a mixture of refined Soltrol 130TM and 1-iodohexadecane. Previous measurements have shown that the iodoheptadecane serves only as the doping phase and does not alter the interfacial tension between the fluids ⁽¹¹⁾. The cores used were Berea sandstones with a diameter of 2.5 cm (1 inch) and a length of about 10 cm (3.9 inches). Porosity measurements made using CT scanner revealed that the cores have porosity in the range of 18 to 21 %. The pressure and temperature were maintained at 800 psi and 25° C for all experiments. These parameters were important to ensure that the displacements were immiscible and also obtain a clear contrast between the fluids in the CT scans. Fluids were injected into cores at constant rates or at rates that were varied to maintain constant pressure. Produced fluids were collected in graduated cylinders. The displacement processes were studied during the experiment where the injection rates, production volumes and pressure drops were measured. Fluid saturation distributions were also indirectly measured using X-Ray CT. The overall efficiency of the process was analyzed by combining the CT measurements and the external effluent volume measurements. A general outline of the experimental procedure is given below:

1. The core is first heated at about 150° F for a sufficient period to remove all residual water saturation and evacuated using a vacuum pump. The evacuated dry core is scanned at a confining pressure of about 1000 psi.
2. For a fractured core experiment, the above steps are repeated after fracturing the core.
3. The core is flooded with CO₂ at the desired temperature and pressure to obtain the scans at 100% CO₂ saturation.
4. The core is then evacuated again in the vacuum chamber. The evacuated core is saturated with doped oil in the vacuum chamber for a period of 48 hours. The oil

saturated core is transferred to the aluminum core holder and about 15 pore volumes of oil are injected to ensure complete saturation.

5. The backpressure regulator at the outlet is fully closed and the pressure in the core holder is allowed to build up. Care is taken that the overburden pressure is always at least 300 psi higher than the pressure inside the sleeve. Once the desired pressure is reached, oil injection is stopped.
6. The oil-saturated core is now scanned again.
7. The pressure in the CO₂ accumulator is increased to be about 50 psi higher than the pressure in the coreflood cell to prevent back flow of oil.
8. CO₂ is now allowed to enter the coreflood cell and any excess pressure above the desired pressure is released using a valve available for this purpose. Injection is then started at the desired rate.
9. The core is scanned at various times to visualize fluid flow and determine saturations at various times.
10. For a WAG experiment, doped/viscosified water is injected when desired and the core is scanned during the injection process. For the experiment with the cross-linker, the gel is injected into the fracture prior to CO₂ injection.

2.4 Results and Discussion

Three types of experiments were performed in this study – Continuous CO₂ injection in unfractured cores, continuous CO₂ injection in fractured cores and CO₂ injection in fractured cores in the presence of viscosified water. For the viscosified water case, experiments were conducted with and without the presence of a cross-linker. A discussion of each of the experiments is given below.

2.4.1 Homogeneous Core Experiments

Two experiments were conducted using homogeneous (unfractured) cores: a high injection rate case where CO₂ was injected at about 1 cc/min and a low injection rate case where CO₂ was injected at 0.03 cc/min. The goal of these two experiments was to investigate bypassing mechanisms at the two injection rates and observe the difference in sweep in the two cases.

High Injection Rate

Fig. 2.2 depicts the cross-sectional scans taken at different times during the experiment. Fig. 2.2a represents the dry core scans with the first scan being the injector end and the last scan being the producer end. In these scans the bright blue color represents regions of high density whereas the dark blue represents regions of low density. The same kind of difference can also be seen in the oil saturated core scans (Fig. 2.2b) where the red color shows regions of high density. Once injection is started, CO₂ can be seen as a blue spot (Fig. 2.2c) and a decrease in the CT number (a number dependent on density, characteristic of a particular material) was observed with an increase in CO₂ saturation (Fig. 2.3). The last set of scans (Fig. 2.2e) taken after about 1 hour of injection show that the core is now almost fully saturated with CO₂. At this point, the produced fluid was only CO₂ and about 95% of the oil had been recovered. However, more than 5 PV of CO₂ had to be injected to obtain this recovery. Fig. 2.4 showing the reconstructions of the cross-sectional images gives a better picture of the fluid flow in the core during CO₂ injection. The injected CO₂ enters the core sweeping most of the oil near the injection port (left) but tends to flow through the center of the core near the producing port (right) hence, bypassing a considerable amount of oil. Continuous injection of CO₂ for a sufficient amount of time allowed CO₂ to contact all regions of the core and squeezed the oil out of those regions. This type of flow commonly occurs in homogeneous cores. However, Fig. 2.4 shows that even in a supposedly homogeneous core, some degree of heterogeneity is still present. The red colored spots on the side of the producing port (right) in Fig. 2.4 represents regions of higher density and lower porosity. It can be seen that the CO₂ flow line thins down at particular regions and remains that way for some time. This phenomenon is also observed in the cross-sectional images and the saturation distributions of CO₂ at different stages, obtained from the scans.

Low Injection Rate

Fig. 2.5 represents the horizontal reconstructions of the cross sectional images at different times, for the low injection rate case. These images clearly depict the effect of injection rate on sweep and utilization of CO₂. It can be seen that at this injection rate, CO₂ does not bypass oil and a very good sweep is obtained. This is because of the fact that there is enough time for CO₂ to diffuse uniformly into all parts of the core. Also, the

breakthrough time of CO₂ reduced considerably compared to the previous case. The effect of heterogeneity in the core is observed to be same as in the previous case. Saturation distributions along the length of the core were obtained from the CT scans. Fig. 2.6 shows the CO₂ saturations from the injector end to the producer end for both the injection rates. It can be seen from the Fig. 2. that breakthrough occurs after about 0.57 PV of CO₂ injection for the low injection rate whereas in the high injection rate case breakthrough occurred at only about 0.3 PV of injection. The Fig. 2. also shows that the final recovery obtained in both cases is consistently above the 90% range, although there is a huge difference in the amount of CO₂ used to obtain such a high recovery. Such a high value of oil recovery obtained even when the displacement is immiscible can be attributed to the light, low viscosity oil used in the experiments. It is important to note that although the sweep in the low injection rate case is very good, the time required to obtain the final recovery value is very high. Hence, one must optimize the injection rate before beginning injection. Fig. 2.7 shows the oil recovery obtained using CT saturations for the two cases.

2.4.2 Fractured Core Experiments

Continuous CO₂ Injection

The permeability of a fracture is typically about 10^3 to 10^6 times greater than the permeability of the porous rock. In a fractured system, the tendency of the fluid would be to flow through the high permeability fracture which leads to early breakthroughs. This phenomenon was observed during CO₂ injection in the fractured core where breakthrough occurred after about 10 minutes of CO₂ injection (0.09 PV). Fig. 2.8 shows the cross-sectional scans of the oil saturated core and the scans at various stages of CO₂ injection. In these scans the color scale has been chosen such that the blues indicate the lowest CT numbers while red and pink indicate the highest CT numbers with green and yellow being the intermediates. Thus, with an increase in CO₂ saturation, the CT number decreases and hence the color changes to a dark shade of blue. From these scans it can be seen that CO₂ moves through the fracture while simultaneously displacing small amounts of oil from the matrix. In such a case there is always some amount of CO₂ that breaks through without contacting any oil, thus greatly reducing the sweep efficiency. The diffusion process is

very slow and given a large amount of time and CO₂, a good recovery may be obtained. In this experiment, the recovery obtained after 2.2 PV of injection is about 58%.

WAG Experiment

In order to prevent early breakthrough of CO₂ and improve sweep efficiency, some kind of conformance control agent is required in the fracture. Although WAG has been the most widely used method for mobility control, its success has not been universal. So, a set of experiments were conducted to analyze the performance of WAG in the presence of fractures. An experiment was first conducted to test water mobility in the core. Brine tagged with both sodium iodide and potassium iodide was used to improve the contrast between the fluids. Water was injected at a rate of about 0.1 cc/min into an oil saturated core. During the experiment we observed that the water mobility in the core was very high and the breakthrough occurred at about 0.4 PV of injection. From the results of this experiment, we concluded that brine by itself cannot delay the breakthrough of CO₂ from the fracture. So we decided to increase the viscosity of water with the aim of reducing its mobility. A conventional WAG process involves alternate injection of specific pore volumes of gas and water to reduce the relative permeability of the gas and hence its mobility. But here, our aim is to delay CO₂ breakthrough and hence we decided to inject the viscosified water into the fracture to “heal” it to some extent so as to reduce CO₂ mobility in fracture. Xanthan was chosen to increase the viscosity of water due to its good injectivity and relative insensitivity of its viscosity to salinity ⁽¹²⁾. Sufficient amount of Xanthan was added to the iodated brine to increase the viscosity to about 20 cp. This was then injected into the core with the injection port aligned with the fracture. Although no problems were encountered with the injectivity of the liquid, we found that once the viscous liquid entered the core, a considerable amount of “leakoff” occurred into the matrix. The main reason for this leakoff is that the cores we used were strongly water wet and imbibition of water into the porous matrix was an extremely quick process. By the time the liquid filled the entire fracture and breakthrough occurred, a considerable quantity had leaked off into the rock and more than 65% of the oil had already been recovered. Fig. 2.9 shows the scans taken at liquid breakthrough where the red color represents the viscous liquid with a higher CT number due to the iodated brine. At this point, liquid injection was stopped and CO₂ injection was started. The liquid remaining in the flow lines was first

displaced into the core by CO₂ and when CO₂ contacted the core, about 80% of the oil had been recovered. This was considered to be the residual oil saturation for the core to water. CO₂ injection resulted in an incremental recovery of about 4.5%. In this case we observed that the breakthrough of CO₂ was delayed considerably due to the presence of the viscous phase. Although the overall recovery obtained was higher than that obtained by continuous CO₂ injection, most of the recovery was due to the viscous water and very little due to CO₂. This again might be due to the strong water-wet nature of the cores used. Using a liquid of higher viscosity (about 30 cp) also gave us similar results. Liquid leakoff into the porous rock can be minimized by using suspended particulate matter ⁽¹³⁾⁽¹⁴⁾. Also, in an oil-wet core, the amount of water imbibing into the porous rock would obviously be lesser and hence the viscous liquid can remain in the fracture, healing it to some extent. But this liquid can still flow and would be produced when CO₂ flows through the fracture. So CO₂ and liquid have to be injected alternately similar to the WAG process. Another method suggested in the literature to minimize leakoff is the addition of a cross-linker to form a gel, when its propagation becomes extremely slow or negligible ⁽¹³⁾.

Experiment with Gel

In this experiment, cross-linked gel was used to delay breakthrough and improve recovery. For this purpose, Guar gum was used with a borate cross linker. Our aim here is not to investigate the use of different gels and any gel that can heal the fracture effectively would serve the purpose. Guar and borate cross linker were chosen because of their easy availability and the gel was formed using this combination. One of the important considerations in using a gel for conformance is the injection pressure. Once the gel is formed by the cross link process, there is a huge increase in the resistance to flow ⁽¹⁵⁾. But Seright ⁽¹³⁾ (1995) proved that gels with low resistance factors can be injected into the fracture without too much “screen out”. Our goal again was not to measure resistance factors. The preformed gel was injected directly into the fracture. A high pressure was required for injection and the pressure drop was about 90 psi/ft. Once the fracture was filled with the gel, a 16 hour setting time was allowed before the start of CO₂ injection. Fig. 2.10 shows the scans taken before the start of injection, at breakthrough and at the end of the experiment with their corresponding ortho reconstructions. It can be observed from the scans that there is a preferential movement of CO₂ in one half of the core compared to

the other. Investigation after the experiment showed that two of the grooves on the injection face were blocked by the gel, on one side. This caused most of the injected CO₂ to flow to the other half of the injection face (open grooves). This also led to a much earlier breakthrough than one would have expected. But it can clearly be observed from the cross sections and the reconstructions that a good sweep has been obtained on both halves of the core. The final recovery in this case was about 95% after approximately 2.5 PV of injection. Fig. 2.11 shows a comparison of the recoveries obtained from the different experiments. It can be observed that the highest recovery is obtained from the experiment using the gel for conformance control.

2.5 Conclusions

Several conclusions can be drawn from this study as follows:

1. Injection rates play an important role in affecting oil recovery and breakthrough.
2. Early breakthrough and higher oil bypass are observed at a high injection rate while low injection rate gives better sweep and lesser utilization of CO₂.
3. Injection rates must be optimized prior to beginning injection.
4. In a fractured system, fluid flow occurs mainly through the fractures. Considerable amount of time is required for the injection fluid to penetrate the matrix and obtain a good recovery.
5. Coreflood experiments using viscosified water confirmed that WAG can delay CO₂ breakthrough and improve recovery. However, leakoff into the porous rock is very high. This leakoff might be much lower in an oil-wet rock but more work is required to establish this.
6. Formation of gel can eliminate the problem of liquid leakoff into the matrix.
7. Using gel for conformance control results in better sweep and higher recoveries. The type and composition of gel to be used in the presence of CO₂ needs more investigation.

2.6 References

1. Yaghoobi, H., Tsau, J.S., Heller, J.P., Improving CO₂ Floods in Heterogeneous Media, paper SPE 35403 presented at the 1996 SPE/DOE Tenth Symposium on Improved Oil Recovery, Tulsa, 21-24 April.
2. Uleberg, K. and Hoier L., Miscible Gas Injection in Fractured Reservoirs, paper SPE 75136 prepared for presentation at SPE/DOE Improved Oil Recovery Symposium, Tulsa, Oklahoma ,April 13-17,2002.
3. Hsie, J.C. and Moore, J.S., The Quarantine Bay 4RC CO₂-WAG Pilot Project: A Post Flood Evaluation, paper SPE 15498 presented at the 1986 SPE Annual Technical conference and Exhibition, New Orleans, 5-8 October.
4. Holm, L.W, O'Brien, L.J., Carbon-Dioxide Test at the Mead-Strawn Field, paper SPE 3103;Journal of Petroleum Technology, pp. 431-432, April 1971.
5. Kane, A.V., Performance Review of a Large-Scale CO₂-WAG Enhanced Recovery Project; SACROC Unit- KELLY SNYDER, JPT 217, Trans., AIME 267, Feb.1979.
6. Aarra, M.G, Skauge, A., Martinsen, H.A., FAWAG: A Breakthrough for EOR in the North Sea, paper SPE 77695 presented at the SPE Annual Technical Conference and Exhibition, San Antonio, TX, September 29 – October2, 2002.
7. Christensen, J.R., Stenby, E.H., and Skauge, A., Review of WAG Field Experience, paper SPE71203; SPE Reservoir Evaluation & Engineering Journal, pp 97-106, April 2001.
8. Frieditis, J., Wolle, C.R. and Notz, P.K., A Laboratory and Field Injectivity Study: CO₂ WAG in the San Andres Formation of the West Texas, paper SPE 22653 presented at the 66th Annual Technical Conference and Exhibition, Dallas, TX, October 6-9.
9. Akervoll, I., Talukdar, M.S., Midtlyng, S.H., Torsaeter, O., WAG Injection Experiments With In-Situ Saturation Measurements at Reservoir Conditions and Simulations, paper SPE 59323 presented at the SPE/DOE Improved Oil Recovery symposium, Tulsa, OK, April 3-5, 2000.
10. Holm, L.W., CO₂ FLOODING: Its Time has Come, paper SPE 11592; Journal of Petroleum Technology, pp. 2739-2745, December 1982.

11. Wellington, S.L. and Vinegar, H.J., X-Ray Computerized Tomography, paper SPE 16983; Journal of Petroleum Technology, pp. 885-898, August 1987.
12. Cannella, W.J., Huh, C. and Seright, R.S., Prediction of Xanthan Rheology in Porous Media, paper SPE 18089 prepared for presentation at 63rd Annual Technical Conference and Exhibition, Houston, October 2-5.
13. Seright, R.S., Gel Placement in Fractured Systems, paper SPE 27740, SPE Production & Facilities Journal pp 241-248, November 1995.
14. Seright, R.S. and Liang, J., A Comparison of Different Types of Blocking Agents, paper SPE 30120 prepared for presentation at the European Formation Damage Conference, The Hague, The Netherlands, May 15-16, 1995.
15. Shahab, H., Jousset, F., Green, D.W., McCool, C.S., Willhite, G.P., Permeability Reduction by a Xanthan/Chromium (III) System in Porous Media , paper SPE 19634; SPERE, pp. 299-304, November 1993.

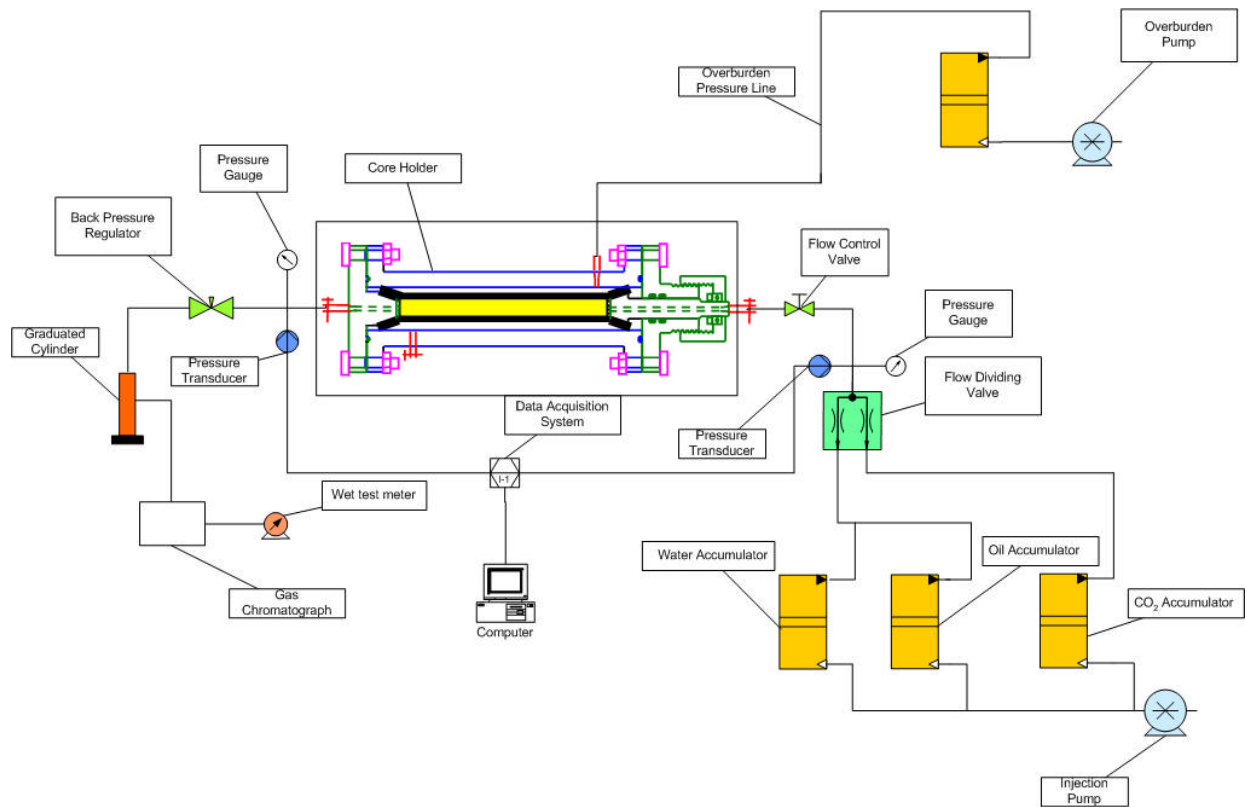
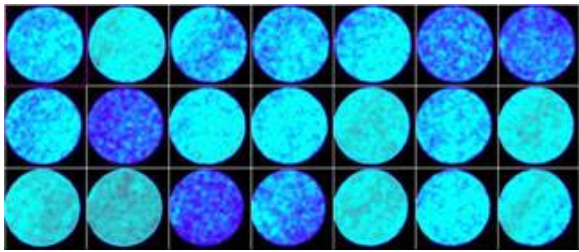
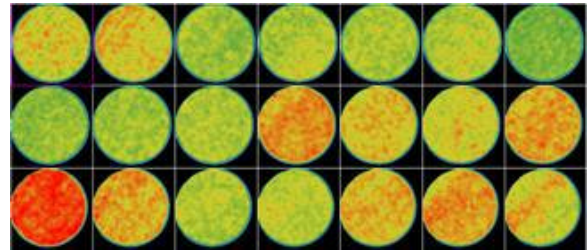


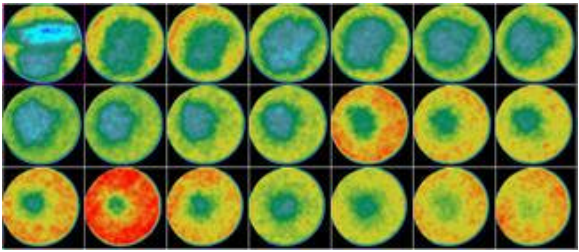
Fig. 2.1 – Schematic of the experimental setup



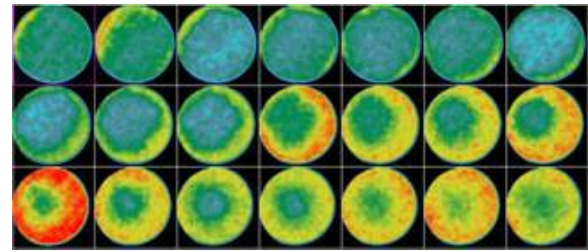
(a) Dry core scans



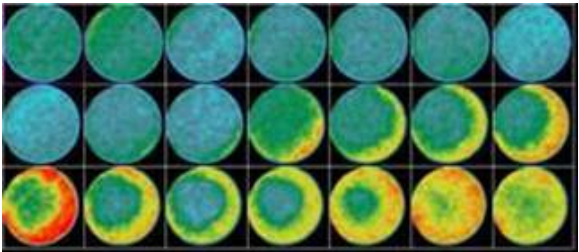
(b) Oil saturated core



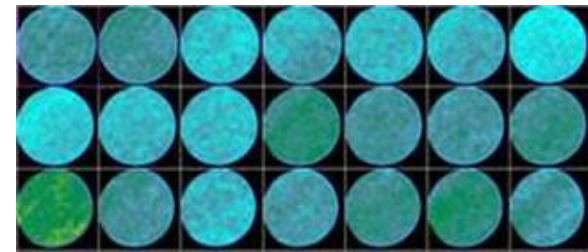
(c) 3 minutes of CO₂ injection



(d) 5 minutes of CO₂ injection



(d) 15 minutes of CO₂ injection



(e) 60 minutes of CO₂ injection

Fig. 2.2 – Cross-Sectional scans taken at various stages during the experiment.

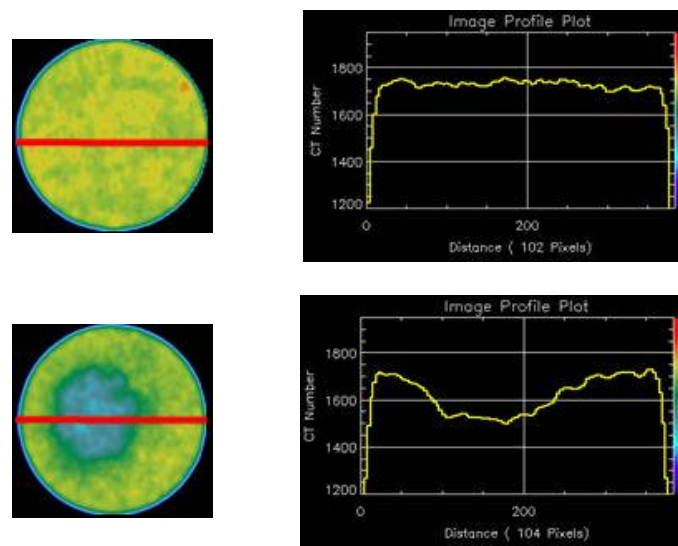


Fig. 2.3 – CT number decreases with increase in CO₂ saturation.

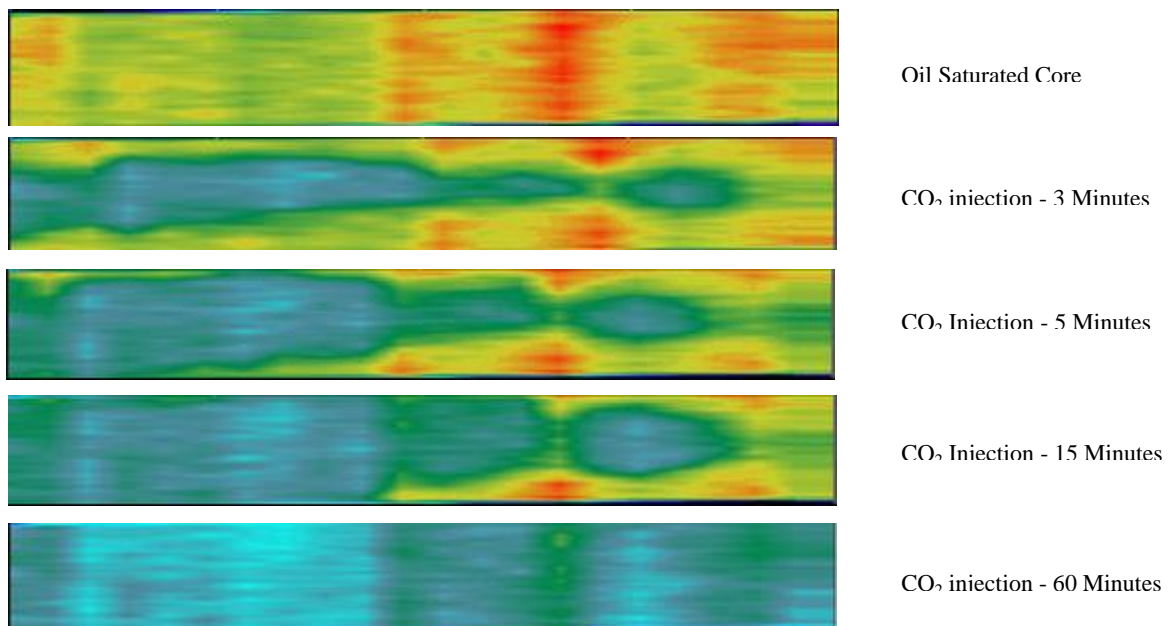


Fig. 2.4 – Reconstructions of cross-sectional scans for high injection rate case.

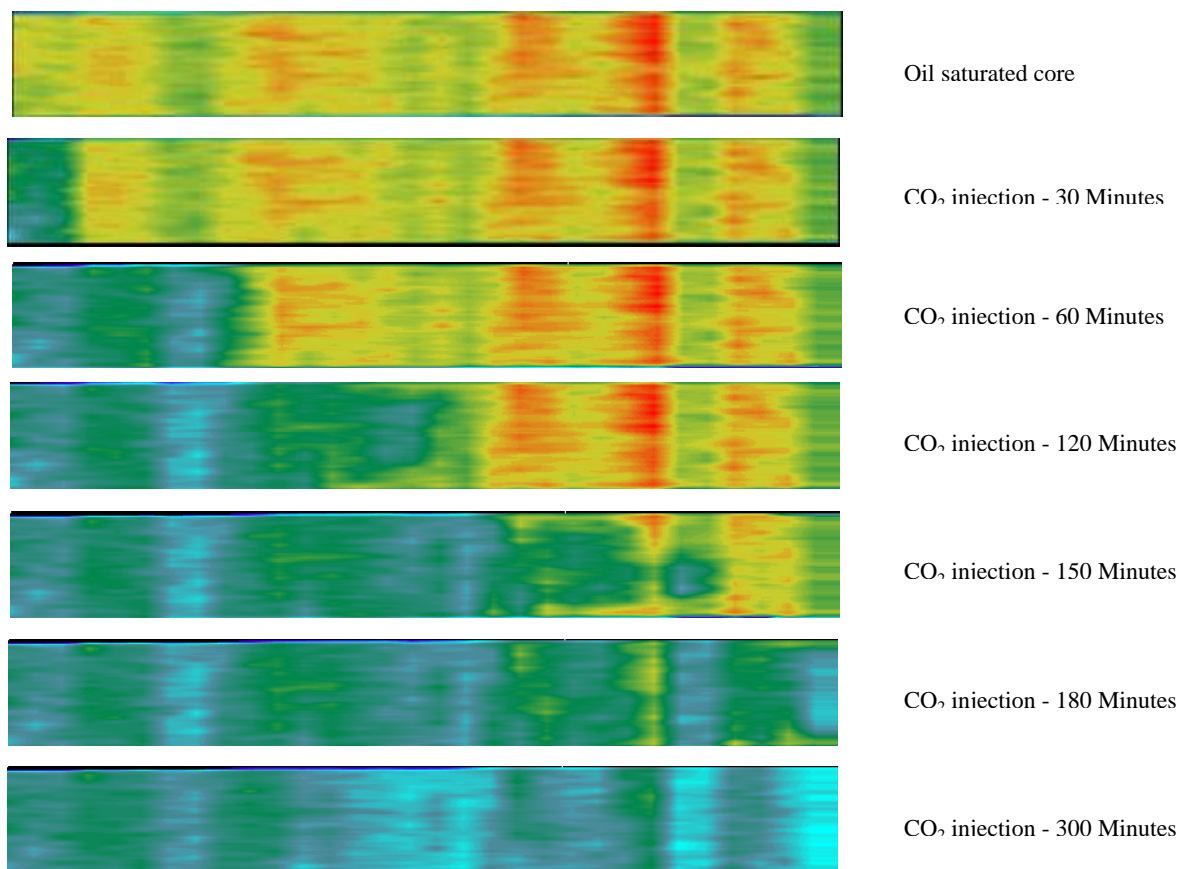
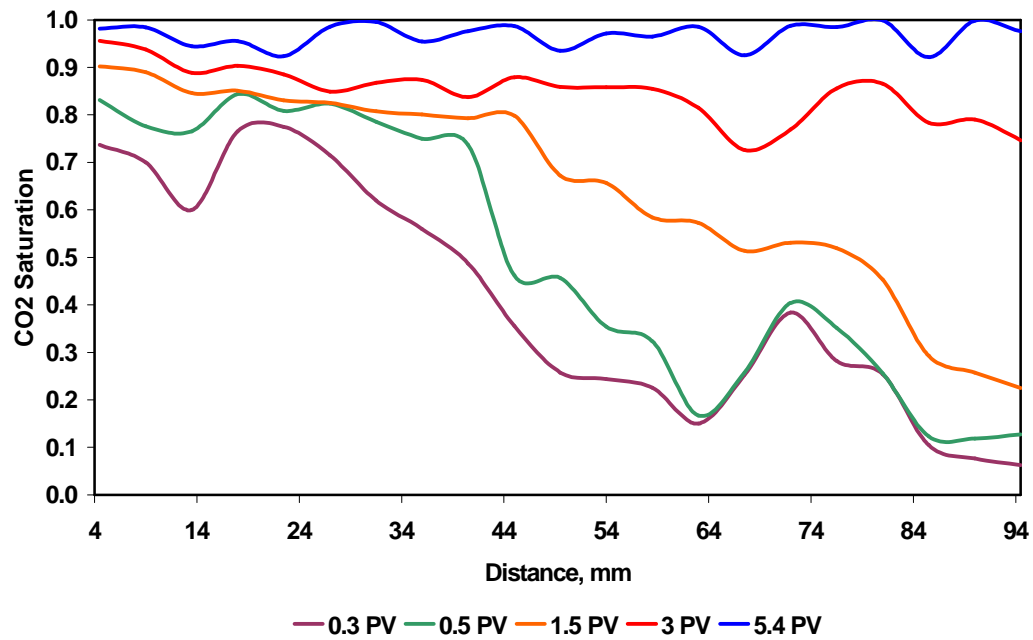
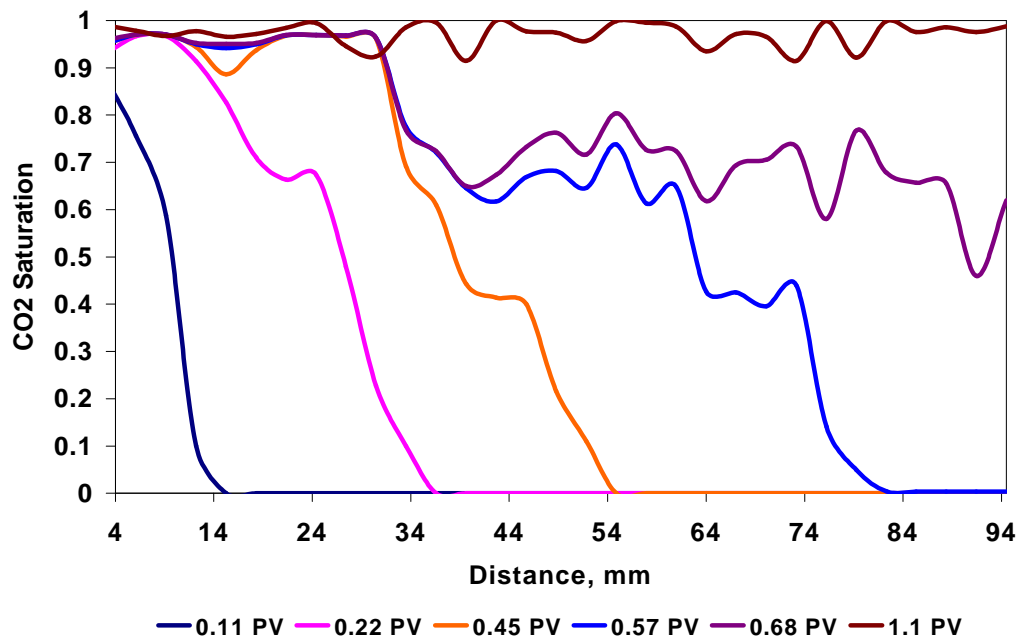


Fig. 2.5 – Reconstructions of cross-sectional scans for low injection rate case shows good sweep.



(a). High injection rate



(b). Low injection rate

Fig. 2.6 – CO₂ saturations along the length of the core at different stages of injection.

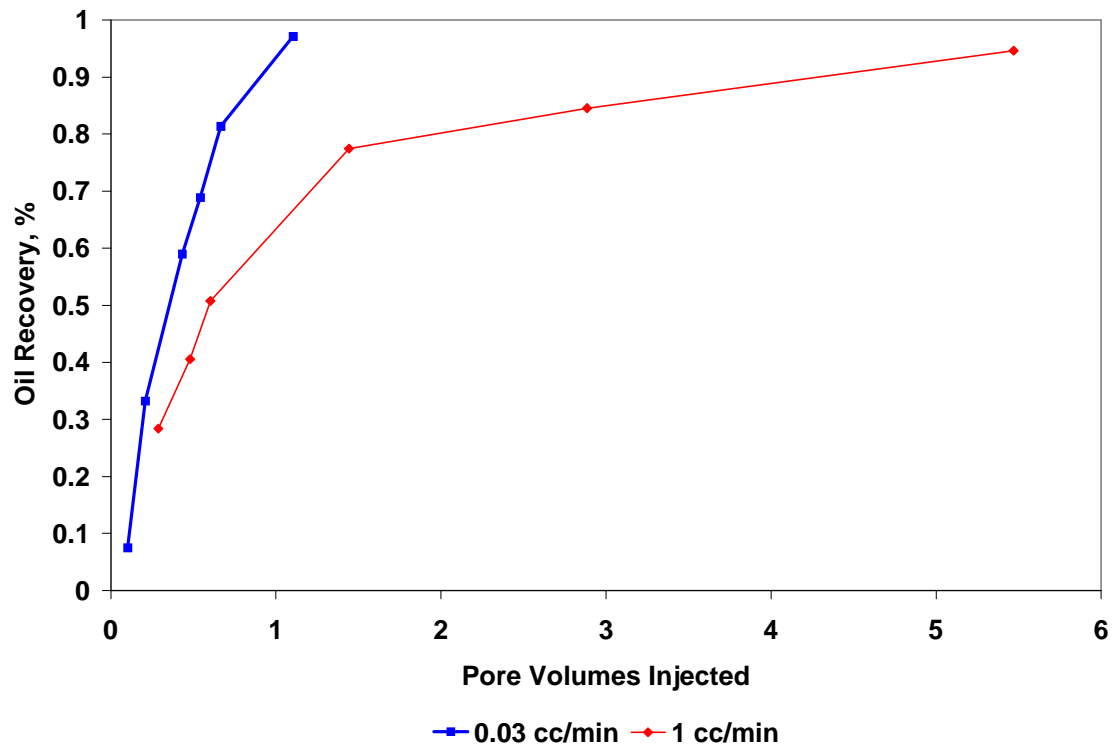
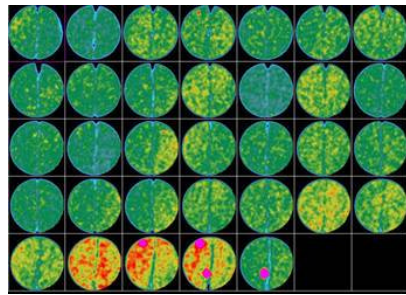
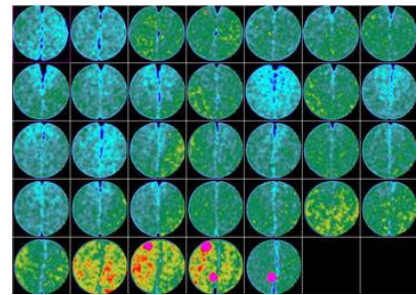


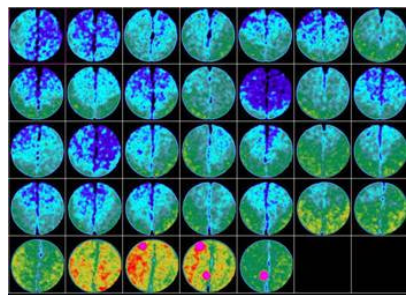
Fig. 2.7 – Higher oil recovery is obtained for lesser pore volumes injected in the low injection rate case



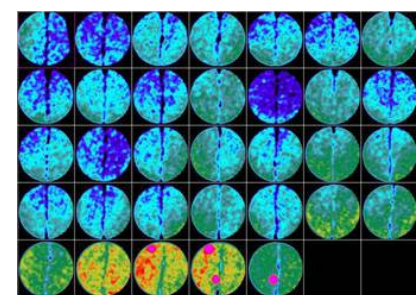
(a). Oil saturated core



(a). CO₂ breakthrough indicated by increase in CO₂ saturation in the fracture

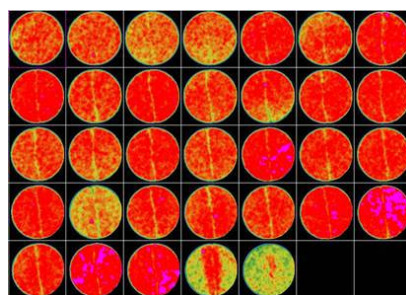


(c). CO₂ saturation after about 1.3 PV of injection

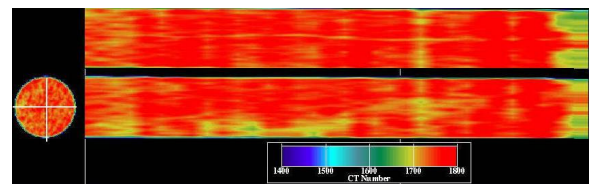


(c). CO₂ saturation at the end of experiment

Fig. 2.8 – Cross-sectional scans taken during the continuous CO₂ injection experiment.

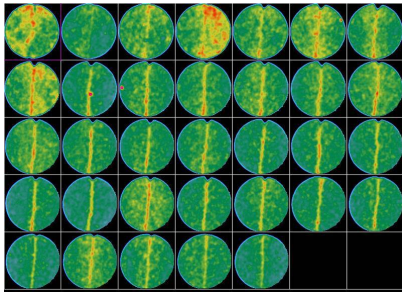


(a). Cross-sectional scans at water breakthrough

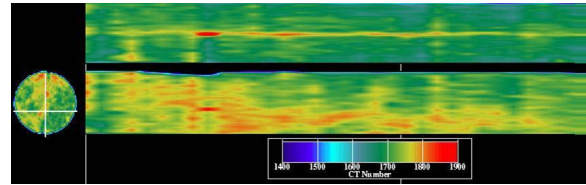


(b). Reconstructions of Cross-sectional scans

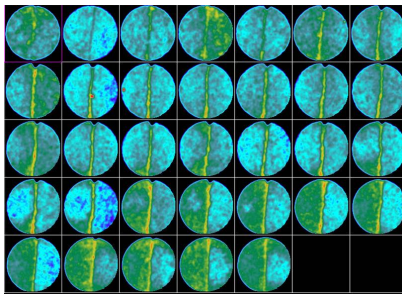
Fig. 2.9 – Scans taken at water breakthrough where red color indicates water.



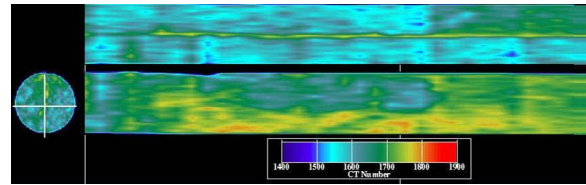
(a). Cross-sectional scans before injection



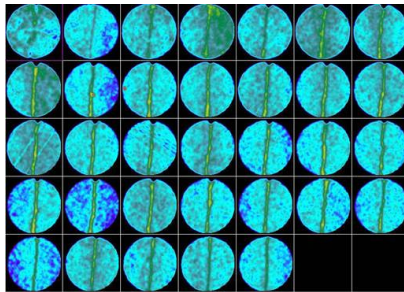
(b). Ortho reconstruction showing gel in the fracture (top) and on the fracture surface (bottom)



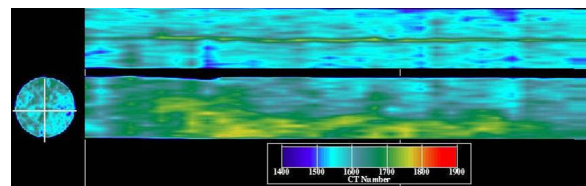
(c). Cross-sectional scans taken at CO₂ breakthrough



(d). Reconstructions of cross-sectional scans showing preferential movement of CO₂ on one half of the core



(e). Cross-sectional scans taken at end of injection



(f). Ortho reconstructions showing gel intact at the end of the experiment

Fig. 2.10 – Scans taken at various stages of the experiment in the presence of gel.

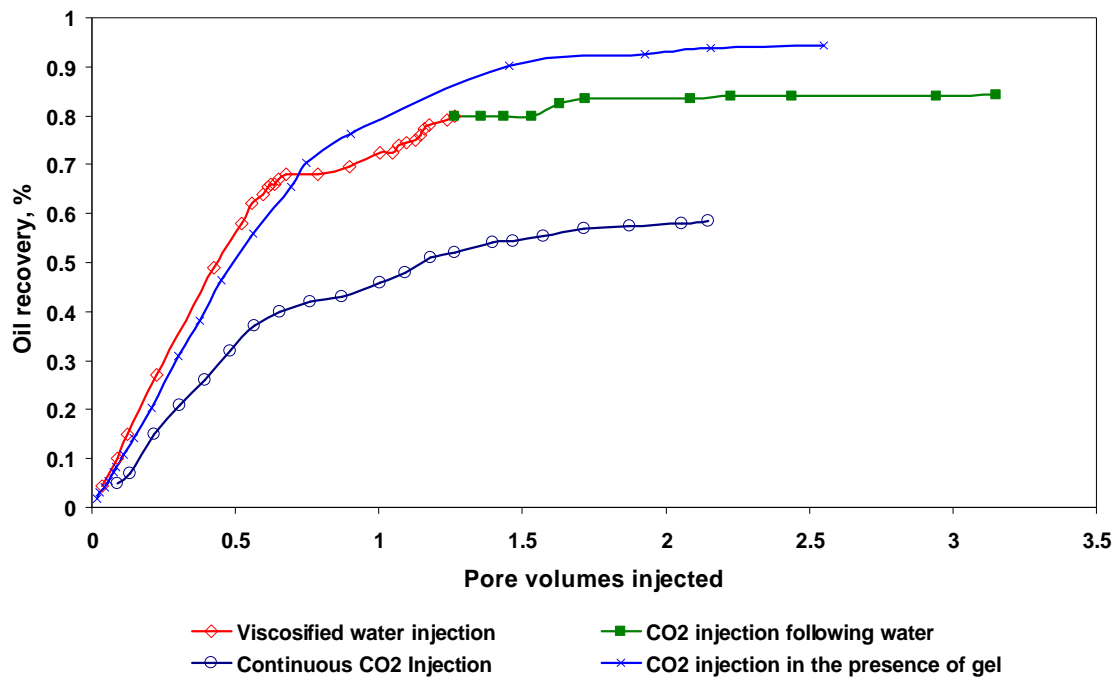


Fig. 2.11 – Recovery curves for the various cases showing highest recovery in the presence of gel.

APPENDIX A: PROJECT FACT SHEET

CONTRACT TITLE: Investigation of Efficiency Improvement During CO ₂ Injection in Hydraulically and Naturally Fractured Reservoirs			
ID NUMBER: DE-FC26-01BC15361 B&R CODE: AC1005000		CONTRACTOR: Texas Engineering Experiment Station ADDR: 322 Wisenbaker Engineering Research Center College Station, TX 77843	
DOE PROJECT MANAGER: NAME: Daniel J. Ferguson LOCATION: NPTO PHONE: 918/ 699-2047 E-MAIL: dan.ferguson@npto.doe.gov		CONTRACT PROJECT MANAGER: NAME: David Schechter PHONE: 979/ 845-2275 FAX: 979/845-1307 E-MAIL: schech@spindletop.tamu.edu	
PROJECT SITE CITY: College Station STATE: TX CITY: STATE: CITY: STATE:		CONTRACT PERFORMANCE PERIOD: 9/28/2001 to 9/27/2004 PROGRAM: Exploration & Production RESEARCH AREA: PRODUCT LINE: ADIS	
CO-PARTICIPANTS:			
PERFORMER:	CITY:	STATE:	CD:
PERFORMER:	CITY:	STATE:	CD:
PERFORMER:	CITY:	STATE:	CD:
PERFORMER:	CITY:	STATE:	CD:

FUNDING (1000'S)	DOE	CONTRACTOR	TOTAL
PRIOR FISCAL YRS	0	0	0
FY 2001 CURRENT OBLIGATIONS	309	78	387
FUTURE FUNDS	628	157	785
TOTAL EST'D FUNDS	937	235	1172

OBJECTIVE: The objective of this project is to perform unique laboratory experiments with Artificial fractured cores (AFCs) and X-ray CT to examine the physical mechanisms of bypassing in HFR and NFR that eventually result in less efficient CO₂ flooding in heterogeneous or fracture-dominated reservoirs. Core flooding experiments in artificially fractured and oil-saturated cores at reservoir conditions will be performed under different conditions of fracture configurations and fracture aperture distributions to investigate matrix-fracture transfer mechanisms. The fluid flow and fracture aperture distributions will be imaged in-situ and real time using X-ray CT. The benefit of WAG in highly heterogeneous reservoirs will be determined. Various CO₂ injection rates, above and below the MMP, will be performed to optimize the operating injection rate and minimize bypassed oil as a result of hydraulic or natural fractures. Numerical analysis will be conducted to model the physical mechanisms of bypassing oil. Results will be important in modeling actual physical mechanisms during CO₂ injection.

PROJECT SUMMARY

Background:

The primary goal of this research is to maximize the potential of CO₂ flooding in the domestic U.S. As more technical knowledge accumulates it becomes clear that natural and hydraulically induced fractures often dominate pattern reservoir or sweep efficiency. As the level of sophistication grows, low permeability reservoirs become more amenable to Enhanced Oil Recovery (EOR) via CO₂. Low permeability reservoirs are usually characterized by brittle matrix rock, which cracks under natural or induced conditions.

Many of the issues involved in saturation distribution during CO₂ injection have been tested in Berea cores above and below miscibility pressure. However, the level of heterogeneity rarely, if ever, includes the presence of natural fractures. This is not coincidental since the level of experimentation required is high in order to develop useful interpretations. The fact remains, however, that reservoir heterogeneity dominates the performance of gas injection. Hydraulic or natural fractures can exert a major influence on the economics of CO₂ injection projects. However, the fundamental mechanisms of transfer in fracture systems are virtually unexplored. The transfer of injected gas from HF or NF determines the ultimate displacement and sweep efficiency. It is the intent of this proposed work to advance the understanding of this dynamic process and determine the implications on the ultimate performance of bypassing reserves during CO₂ injection.

Work to be performed:

Task 1.0 Experimental Investigation of Transfer Mechanisms during CO₂ Flooding in NFR and HFR.

1. Laboratory results to demonstrate the effect of overburden pressure (stress-state) on fracture aperture distribution and permeability of the rock (level of heterogeneity).
2. Effect of fracture aperture distribution on viscous and capillary forces.
3. Laboratory results to demonstrate the effect of hydraulic fracture on sweep efficiency and fracture-matrix interactions.

Task 2.0 Experimental Investigation of Bypassing Mechanisms during CO₂ Flooding in HFR and NFR.

1. Laboratory results showing optimum WAG injection ratio that maximizes the sweep efficiency.
2. Laboratory results showing optimum injection rate that mitigates bypassing oil reserve during CO₂ injection in HFR and NFR.
3. Possible strategies to mitigate bypassing mechanisms that will result in less bypassing and more efficient CO₂ flooding in fracture-dominated reservoirs.

Task 3.0 Imaging Experiments Using X-ray CT.

1. Imaging the saturation profile of non-fractured and fractured cores for investigating bypassing mechanisms and modeling purpose

Task 4.0 Analysis and Modeling Transfer and Bypassing Mechanisms.

1. Development of mathematical model and/or numerical modeling to examine the physical mechanisms of bypassing that occur in hydraulically and naturally fractured reservoirs, both above and below the MMP.
2. Identifying important parameters affecting bypassing mechanisms.
3. Providing more confident scaling of field performance from laboratory experiments.

ACCOMPLISHMENTS:

Task 1.0 Literature Review

Task 2.0 Experimental Investigation of Transfer Mechanisms during CO₂ Flooding in NFR and HFR.

1. Laboratory results to demonstrate the effect of overburden pressure (stress-state) on unfractured and fractured cores. Quantification of flow path contributors (matrix or fracture) and determination of fracture aperture (width) and matrix and fracture permeability under variable overburden pressures and injection rates.
2. Laboratory results to demonstrate the effect of overburden pressure (stress-state) on unfractured and fractured cores in multiphase flow. The preliminary results of static imbibition experiments are presented as a precursor to image the saturation profiles of non-fractured and fractured cores using X-Ray CT scanner.

3. Establish the fracture aperture calibration.
4. Laboratory results to demonstrate the effect of overburden pressure (stress-state) on fracture aperture distribution and permeability of the rock (level of heterogeneity).
5. Development dual porosity simulator using empirical transfer function.
6. Laboratory results showing optimum WAG injection ratio that maximizes the sweep efficiency.
7. Laboratory results showing optimum injection rate that mitigates bypassing oil reserve during CO₂ injection in HFR and NFR.
8. Possible strategies to mitigate bypassing mechanisms that will result in less bypassing and more efficient CO₂ flooding in fracture-dominated reservoirs.

Task 3.0 Imaging Experiments Using X-ray CT.

1. Imaging the saturation profile of non-fractured and fractured cores at spontaneous experiments for investigating fluid intake (capillary force) and for modeling spontaneous imbibition.
2. Imaging the movement of brine in oil saturated core.
3. Imaging the movement of brine in a fractured core horizontally and vertically for verifying the use of parallel plate model.
4. Imaging the fractured core for establishing fracture aperture calibration.
5. Imaging the fractured cores for examining fracture aperture distribution under different overburden pressure.
6. Imaging the saturation profile of non-fractured and fractured cores for investigating bypassing mechanisms during CO₂ flooding.
7. Imaging the polymer gels to mitigate bypassing mechanisms that will result in less bypassing and more efficient CO₂ flooding in fracture-dominated reservoirs.

Task 5.0 Analysis and Modeling Transfer and Bypassing Mechanisms.

1. Modeling the laboratory experiment to investigate of the effect of fracture aperture at variable overburden pressures.
2. Modeling fluid flow through a single fracture using experimental, stochastic and simulation approaches to investigate the effect of different rock heterogeneity on flow path contributors.
3. Validation of cubic law equation.
4. Modeling study to investigate the effect of different rock heterogeneity on flow path contributors.
5. Modeling study to investigate the transfer mechanism during core flooding in fractured core.




PROJECT STATUS




Current Work:

Task 5.0 Analysis and Modeling Transfer and Bypassing Mechanisms.

1. Modeling CO₂ flooding in non-fractured and fractured cores

SCHEDULED MILESTONES:

	Time (months)						
	0	6	12	18	24	30	36
Task 1. Literature Review							
Task 2. Experimental Investigation of Transfer Mechanisms during CO ₂ Flooding in NFR and HFR							
Task 3. Experimental Investigation of Bypassing Mechanisms during CO ₂ Flooding in HFR and NFR							

Task 4. Imaging Experiments Using X-ray CT	
Task 5. Analysis and Modeling Transfer and Bypassing Mechanisms	
Task 6. Technology Transfer	

 Accomplished Milestones
 Proposed Milestones

REPORTS:

Putra, E., Schechter, D.S., and Vivek, M.: “Effect of Overburden Pressure on Unfractured and Fractured Permeability Cores,” report included in “Investigation of Efficiency Improvement during CO₂ Injection in Hydraulically and Naturally Fractured Reservoirs” First Semi-Annual Progress Report (DOE Contract No.: DE-FC26-01BC15361), Oct 2001-March 2002.

Alfred, D., Muralidharan, V., Putra, E., and Schechter, D.S.: “Modeling Fluid Flow through Single Fracture Using Experimental, Stochastic and Simulation Approaches,” report included in “Investigation of Efficiency Improvement During CO₂ Injection in Hydraulically and Naturally Fractured Reservoirs” Second Semi-Annual Progress Report (DOE Contract No.: DE-FC26-01BC15361), April 2002-October 2002.

Muralidharan, V., Putra, E., and Schechter, D.S.: “Investigating the Changes in Matrix and Fracture Properties and Fluid Flow under Different Stress-state Conditions,” report included in “Investigation of Efficiency Improvement During CO₂ Injection in Hydraulically and Naturally Fractured Reservoirs” Second Semi-Annual Progress Report (DOE Contract No.: DE-FC26-01BC15361), April 2002-October 2002.

Muralidharan, V., Kaul S., Putra, E., and Schechter, D.S.: “Preliminary Results of Imaging Imbibition Process Using X-Ray CT Scanner,” report included in “Investigation of Efficiency Improvement during CO₂ Injection in Hydraulically and Naturally Fractured Reservoirs” Second Semi-Annual Progress Report (DOE Contract No.: DE-FC26-01BC15361), April 2002-October 2002.

Kaul, S., Putra, E., and Schechter, D.S.: “X-Ray Tomography Results Validate Numerical Modeling of Flow in Fractures,” report included in “Investigation of Efficiency Improvement during CO₂ Injection in Hydraulically and Naturally Fractured Reservoirs,” Third Semi-Annual Progress Report (DOE Contract No.: DE-FC26-01BC15361), October 2002-March 2002.

Tellapaneni, P.K., Putra, E., and Schechter, D.S.: “Simulation of Naturally Fractured Reservoirs Using Empirically Derived Transfer Function,” report included in “Investigation of Efficiency Improvement during CO₂ Injection in Hydraulically and Naturally Fractured Reservoirs,” Fourth Semi-Annual Progress Report (DOE Contract No.: DE-FC26-01BC15361), April 2003-October 2003.

Muralidharan, V., Chakravarthy D., Putra, E., and Schechter, D.S.: “Fracture Aperture and Fracture Distribution,” report included in “Investigation of Efficiency Improvement during CO₂ Injection in Hydraulically and Naturally Fractured Reservoirs” Fourth Semi-Annual Progress Report (DOE Contract No.: DE-FC26-01BC15361), April 2003-October 2003.

Chakravarthy D., Muralidharan, V., Putra, E., and Schechter, D.S.: “Application of X-Ray CT for Investigating Effect of CO₂ Injection Rates on Oil Recovery,” report included in “Investigation of Efficiency Improvement during CO₂ Injection in Hydraulically and Naturally Fractured Reservoirs” Fifth Semi-Annual Progress Report (DOE Contract No.: DE-FC26-01BC15361), Nov 2003-March 2004.

Chakravarthy D., Muralidharan, V., Putra, E., and Schechter, D.S.: "Possible Strategies to Mitigate CO₂ Flooding Bypassing Mechanisms in Fracture-Dominated Reservoirs," report included in "Investigation of Efficiency Improvement during CO₂ Injection in Hydraulically and Naturally Fractured Reservoirs" Fifth Semi-Annual Progress Report (DOE Contract No.: DE-FC26-01BC15361), Nov 2003-March 2004.

TECHNOLOGY TRANSFER ACTIVITIES:

Presentations

On April 17-21, 2004, we presented the talk, "Modeling Fluid Flow through Single Fractures Using Experimental, Stochastic and Simulation Approaches," for SPE/DOE 89442 at 2004 Improved Oil Recovery Symposium, OK.

On March, 2004, we (Vivek Muralidharan) presented the talk, "Simulation and Imaging Experiments of Fluid Flow through a Fracture Surface: A New Perspective," for 2004 Student Research Week Competition in Texas A&M University and won the first place.

On February 16, 2004, we (Vivek Muralidharan) presented the talk, "Simulation and Imaging Experiments of Fluid Flow through a Fracture Surface: A New Perspective," for 2004 SPE Texas A&M contest and won first place in first round and 1st place in final round MS division of Texas A&M. Vivek represented Texas A&M at Regional Region at Texas Tech University, April 2004 and won first place. He will compete in International Region at 2004 SPE Annual Meeting, Houston and at Calgary University, Canada, June 2004.

On February 16, 2004, we (Deepak Chakravarthy) presented the talk, "Application of X-Ray CT to Investigate Effect of Rock Heterogeneity and Injection Rates during CO₂ Flood Process," for 2004 SPE Texas A&M contest and won first place in first round MS division of Texas A&M. Deepak will represent Texas A&M at International Region at Calgary University, Canada, June 2004.

On February 16, 2004, we (Emeline Chong) presented the talk, "Development of a Reservoir Simulator with Unique Grid-Block System," for 2004 SPE Texas A&M contest and won second place in first round MS division of Texas A&M.

On February 16, 2004, we (Orkhan H Pashayev) presented the talk, "Imbibition Assisted Recovery," for 2004 SPE Texas A&M contest and won third place in first round MS division of Texas A&M.

On February 16, 2004, we (Prasanna K Tellapaneni) presented the talk, "Usage of X-ray CT in Dual Porosity Simulation," for 2004 SPE Texas A&M contest and won second place in first round PhD division of Texas A&M.

On September 18, 2003, we presented the talk "Waterflood and CO₂ performance in the Naturally Fractured Spraberry Trend Area," at the Statoil Research Summit 2003, Trondheim, Norway.

On February 8, 2003, we (Dicman Alfred) presented the talk, "Modeling Flow through Fractures using Experimental, Stochastic and Simulation Approaches," for 2003 SPE Texas A&M contest and won 2nd place in first round and 1st place in final round MS division of Texas A&M. Dicman represented Texas A&M at Regional Region at Rice University and International Region at Calgary University, Canada and won 2nd place at both regions.

On February 8, 2003, we (Sandeep P. Kaul) presented the talk, "X-Ray Tomography Results Validate Numerical Model of Flow in Fractures," for 2003 SPE Texas A&M contest and won 2nd place in first round MS division of Texas A&M.

On February 8, 2003, we (Vivek Muralidharan) presented the talk, "overburden pressure affects fracture aperture and fracture permeability in a fractured reservoir," for 2003 SPE Texas A&M contest and won 2nd place in first round MS division of Texas A&M.

On June 2003, we presented the Short Course for Saudi Aramco in Al Khobar, Saudi Arabia – “Reservoir Characterization, Engineering and Enhanced Oil Recovery in Naturally Fractured Reservoirs.”

On March 2003, we presented the Short Course for UNAM/PEMEX in Mexico City, Mexico – “Reservoir Characterization and Engineering in Naturally Fractured Gas and Oil Reservoirs – Part II.”

On June 13, 2002, we presented the "Imbibition and its Relevance to Waterflood Performance in the Naturally Fractured Spraberry Trend Area," at the Rice University and University of Houston invited lecture for Society of Petroleum Engineering Chapter, Duncan Hall, Rice University.

On October 2001, we presented the Short Course for UNAM/PEMEX (National Petroleum Company of Mexico) in Mexico City, Mexico – “Reservoir Characterization and Engineering in Naturally Fractured Gas and Oil Reservoirs - Part I.”

On February 2001, we presented the Short Course for UNAM/PEMEX in Mexico City, Mexico – “Reservoir Characterization and Engineering in Naturally Fractured Gas and Oil Reservoirs – Part I.”

Papers and Publications

1. Chong, E., Syihab, Z., Putra, E. and Schechter, D.S.: “A Unique Grid-Block System for Improved Grid Orientation,” paper SPE 88617 will be presented at 2004 Asia Pacific Oil and Gas Conference and Exhibition (APOGCE), Perth, Australia, 18-20 October.
2. Muralidharan, V., Putra, E., and Schechter, D.S.: "Experimental and Simulation Analysis of Fractured Reservoir Experiencing Different Stress Conditions," paper CIPC 2004-229 will be presented at 2004 Annual Technical Meeting of the Petroleum Society, Calgary, Canada, 8-10 June.
3. Muralidharan, V., Chakravarthy, D., Putra, E., and Schechter, D.S.: "Investigating Fracture Aperture Distributions under Various Stress Conditions Using X-Ray Scanner," paper CIPC 2004-230 will be presented at 2004 Annual Technical Meeting of the Petroleum Society, Calgary, Canada, 8-10 June.
4. Chakravarthy, D., Muralidharan, V., Putra, E., and Schechter, D.S.: "Application of X-Ray CT for Investigating CO₂ and WAG Injection in Fractured Reservoirs," paper CIPC 2004-232 will be presented at 2004 Annual Technical Meeting of the Petroleum Society, Calgary, Canada, 8-10 June.
5. Tellapaneni, P.K., Putra, E., and Schechter, D.S.: "Usage of X-Ray CT for Empirical Transfer Functions in Dual Porosity Simulation," paper CIPC 2004-246 will be presented at 2004 Annual Technical Meeting of the Petroleum Society, Calgary, Canada, 8-10 June.
6. Kaul, S.P., Putra, E., and Schechter, D.S.: "Simulation of Spontaneous Imbibition Using Rayleigh-Ritz Finite Element Method-A Discrete Fracture Approach," paper CIPC 2004-228 will be presented at 2004 Annual Technical Meeting of the Petroleum Society, Calgary, Canada, 8-10 June.
7. Alfred, D., Putra, E., and Schechter, D.S.: "Modeling Fluid Flow through Single Fractures Using Experimental, Stochastic and Simulation Approaches," paper SPE/DOE 89442 will be presented at 2004 Improved Oil Recovery Symposium, OK, Tulsa, 17–21 April.
8. Alfred, D., Putra, E., and Schechter, D.S., Modeling Fluid Flow Through a Single Fracture Using Experimental, Stochastic and Simulation Approaches, accepted for publication, Saudi Aramco Journal of Technology, Spring, 2004.
9. Putra, E., Muralidharan, V., and Schechter, D.S., Overburden Pressure Affects Fracture Aperture and Fracture Permeability in a Fractured Reservoir, accepted for publication, Saudi Aramco Journal of Technology, Fall 2003.
10. Kaul, S.P., Putra, E., and Schechter, D.S.: “X-Ray Tomography Results Validate Numerical Modeling of Flow in Fractures,” Jurnal Teknologi Mineral, 2003

Internet Postings on the Project and Software to Download

A description of our research group can be found at the following Petroleum Engineering Texas A&M Website: <http://pumpjack.tamu.edu/faculty/schechter/baervan/homepage.html>. The site lists the publications of our group and allows downloads of several papers, reports, and presentations.

This website also allows downloading of software, i.e. spontaneous imbibition simulator, Delaunay Triangulation, reservoir management software (in progress) and reservoir modeling simulator (in progress).

CONTRACT INFORMATION:

NAME: David Schechter

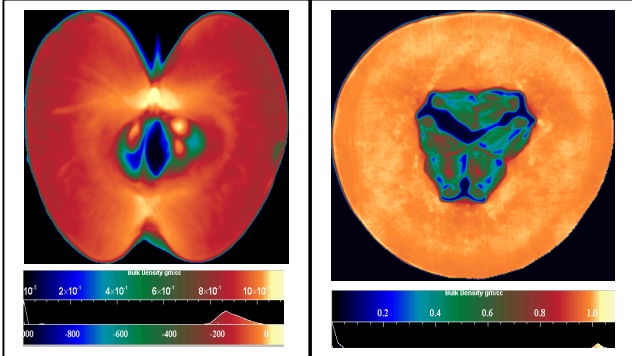
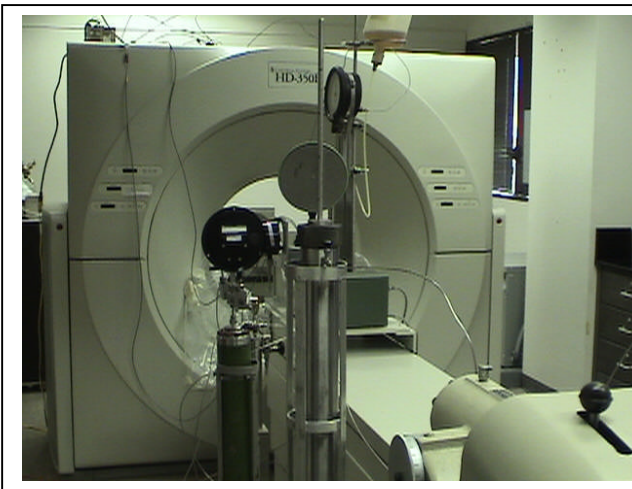
PHONE: 979/ 845-2275

FAX: 979/845-1307

E-MAIL: schech@spindletop.tamu.edu

DIGITAL PICTURES:

X-Ray CT Scanner Laboratory



The CT Scanner can be used to measure porosity and fluid saturations; to identify phase types and interfaces; and to determine the presence of mineral types and fractures in formation cores. The CT scanner uses the same principle as the basic x-ray. Inside the scanner is a round rotating frame which has x-ray tube mounted on one side and a curved detector on the opposite side. As the frame rotates 360 degrees around the object, a fan of x-rays go through the object to the detector on the opposite side producing a slice image on the digital computer. Measured values are stored as two-dimensional pixel images, which may be combined to create a three-dimensional image of the object scanned.

The CT Scanner uses the combination of the digital computer and rotating x-ray devices to create detailed cross sectional images. The CT Scanner was initially developed and predominantly used as a medical diagnostic tool. With the advent of high-resolution scanners and powerful imaging software has made the CT Scanner increasingly more important as a research and diagnostic tool in petroleum industry.

The HD 350 X-Ray CT Scanner (Fourth Generation) is a state-of-the-art CT scanner capable of scanning objects as large as 50 cm in diameter at scan speeds of 2 seconds per revolution. Acquired in October 2002, the scanner has a cross-sectional resolution of 0.3 mm by 0.3 mm and a fully programmable sample positioning table with a travel precision of 0.03 mm.

To date, the CT Scanner has been used in research projects supported by the U.S Department of Energy for identification fractures and vugs in formation cores, measurement of fracture apertures under different overburden pressure and fluid saturation in fractured cores during waterflood experiments. The CT scanner also is an invaluable research tool for research in other disciplines whenever high-resolution noninvasive diagnostics and measurements are required.

